

TRACER BEHAVIOUR IN PIPELINES WITH DEPOSITS AND ANALYSIS OF NATURAL GAS PRESSURE FUNCTIONS

Diploma Thesis Work



By
Salako Abiodun Ebenezer

Supervised by:
Prof. J. S. Gudmundsson

Department of Petroleum Engineering &
Applied Geophysics
Norwegian University of Science and Technology
Trondheim
Norway



Trondheim
July 2006

NTNU

**Norges teknisk-naturvitenskapelige
universitet**

Studieprogram i Geofag og petroleumsteknologi

Study Programme in Earth Sciences and Petroleum Engineering

Fakultet for ingeniørvitenskap og teknologi

Faculty of Engineering and Technology



**Institutt for petroleumsteknologi og anvendt geofysikk
Department of Petroleum Engineering and Applied Geophysics**

HOVEDOPPGAVEN/DIPLOMA THESIS/MASTER OF SCIENCE THESIS

Kandidatens navn/ The candidate's name: Salako Abiodun Ebenezer

Oppgavens tittel, norsk/Title of Thesis, Norwegian:

Oppførsel Av Tracer i Rørledinger med Utfellinger og Analyse av Trykkfunksjoner for Naturgass

Oppgavens tittel, engelsk/Title of Thesis, English:

Tracer Behaviour in Pipeline with Deposits and Analysis of Natural Gas Pressure Functions

Utfyllende tekst/Extended text:

Behavior of tracer flowing in pipelines would be analyzed and its application to evaluate the amount of deposits in a pipeline of about 100 km and 6 – 8 inches internal diameters. An established mathematical model base on Taylor dispersion theory would be used to analyze this behavior.

The application of tracer technology to estimate the liquid accumulation in pipeline would also be carried out.

Secondary task of this thesis is to analyze the pressure functions of natural gas. The effect of natural gas PVT properties such as molecular weight and gas specific gravity would be investigated and the effect of temperature on pressure functions would also be presented.

Studieretning/Area of specialization: Production Engineering

Fagområde/Combination of subjects: Petroleum Technology

Tidsrom/Time interval:

.....
*Jon Steinar Gudmundsson
Faglærer/Teacher*

Declaration

I **Salako Abiodun Ebenezer** declared that this thesis work was carried out by me in accordance with Norwegian University of Science and Technology rules and regulations

.....
Date

.....
Signature

Abstract

Deposits in pipelines are a serious field problem encountered during oil and gas production. Deposits cause plugging, and reduction in pipeline capacity/hydraulic diameter. For optimal operations of pipelines, there is need to estimate the amount of deposits in pipelines to enable a cleaning program to be effectively devised.

The primary aim of this Thesis is to present a chronological methodology on how tracer technology can be used to estimate the amount of deposits in sub-sea pipelines. An established mathematical model based on Taylor's theory of dispersion in a pipe flow was presented to generate the concentration-time profile of tracer flowing through a given pipeline of about 100 km long and 6-8 inches in diameter, a simple measurement of tracer pulse velocity is obtained by dividing the time of flight of the pulse by the total distance travelled. Given that the flow rate through the pipeline is known, the effective cross-sectional area is estimated and hence the volume of the pipeline deposits.

Relationship between deposits thickness and the corresponding changes in the pipeline diameter model is derived to establish the effect of flow measurement accuracy on the minimum amount of deposit thickness that can be detected. The tracer technology is based on measurement of effective internal diameter of the pipeline and its accuracy is dependent on the accuracy of fiscal flow meter.

Liquid-loading in multiphase flow in pipeline using tracer dilution mass flow measurement method was also carried out. Application of the method based on field experience shows that liquid accumulation estimate for pipeline in flat terrain to be reasonably accurate, while hilly terrain shows some deviations.

The secondary task of this thesis is to present the pressure functions of natural gas at high temperature and high pressure (HTHP) as found in the North Sea. Different natural gas compositions are analyzed using HYSYS process simulator to estimate the PVT properties of the gases. The pressure function obtained for gas composition with specific gravity in the range of 0.554 – 0.67 is linear at low pressure (≤ 110 bars) and non-linear at high pressure. Gas composition with specific gravity greater than [1] is non-linear at low pressure and constant at high pressure. The temperature shift the functions upwards at low pressure range, while at high pressure the pressure functions shift downward as the temperature decreases.

Acknowledgements

I wish to express my sincere appreciation to my Supervisor Professor Jon Steinar Gudmundsson for his unalloyed support, advice, and guidance during the course of writing this thesis.

I also wish to thank some of my class mate for their contributions one way or the other in order to make this thesis a successful one.

Special thanks to NORAD Scholarships award for given me the opportunity to study here in Norway.

Lastly to my parents for there moral support, I will always be grateful for their loving kindness.

List of Contents

Declaration	iii
Abstract	iv
Acknowledgements	v
List of Contents	vi
List of Tables.....	viii
List of Figures	ix
Nomenclature	x
1 Introduction	1
2 Taylor Dispersion in Pipeline.....	3
2.1 Dispersion Model	3
2.2 Mechanisms of Dispersion	4
2.2.1 Molecular Diffusion	4
2.2.2 Taylor Dispersion.....	5
2.3 Dispersion Regimes.....	5
2.4 Dispersion Coefficient.....	6
2.4.1 Longitudinal Dispersion Coefficient.....	7
3.0 Deposit Formations in Pipeline	9
3.1 Wax Depositions	9
3.1.1 Molecular Diffusion	9
3.1.2 Other Proposed Mechanisms.....	10
3.2 Hydrate Depositions	11
3.3 Asphaltene Depositions.....	11
3.4 Scale Depositions	13
3.4.1 Incompatible Mixing	14
3.4.2 Auto-scaling	14
4 Pipeline Deposits Evaluation Techniques	15
4.1 Pressure Pulse Techniques	15
4.2 Pressure Drop Technology	16
4.3 Pigging Technology	16
4.4 Thermal Technology	17
4.5 Spool Piece Technology.....	17
5 Tracer Technology	18
5.1 Tracer Flow Concentration Profiles	18

5.2	Tracer Transit Time.....	19
5.3	Tracer Mean Velocity.....	19
5.4	Effect of pipe Roughness on Tracer Flow.....	19
5.5	Flow Rate Measurement Sensitivity on Tracer Testing.....	20
5.6	Estimation of Deposits in Pipeline.....	20
5.7	Estimation of Liquid Loading in Pipeline.....	20
6.0	Pressure Function for Gas Wells.....	23
6.1	Gas Pressure Function at High Temperature and Pressure.....	23
6.2	Effect of Fluid Properties on Pressure Functions.....	23
7	Discussions of Results.....	25
7.1	Effective Internal Pipeline Diameter.....	25
7.2	Effect of Pipeline Roughness on Tracer Flow.....	26
7.3	Sensitivity of Tracer Testing on Flow Rate Measurement.....	26
7.4	Effect of Gas Specific Gravity on Pressure Function.....	26
7.5	Effect of temperature on Pressure Functions.....	27
8.0	Conclusions.....	28
	Reference:.....	29
	Figures:.....	32
	Tables:.....	47
	Appendices.....	51
Appendix A:	Tracer Concentration Response Calculation in pipeline.....	51
Appendix B:	Flow Rate Sensitivity on Tracer Testing Calculation.....	53
Appendix C:	Pressure Functions Calculations.....	55

List of Tables

Table 1	Range of values for Diffusion and Dispersion Coefficients	6
Table 2	Flow Rate Accuracy for Different Flow Meters (Marlin 2006).....	47
Table 3	Frigg Produced gas Composition (Maritvold, 1990).	48
Table 4	Sleipner Produced gas Composition (Gudmundsson Lecture note, 2005)	49
Table 5	Shtokmanskoye Produced gas Composition	49
Table 6	Processed Gas compositions Mole % for different gas Field	50
Table 7	Tracer Response Sample Calculation.....	52
Table 8	Concentration response at different locations along the pipeline	52
Table 9	Calculation of changes in Pipeline Area with Deposit Thickness	54
Table 10	Pressure Function Calculation for Frigg gas and Methane	55
Table 11	Pressure Function Calculation for Sleipner gas Field and Shtokman Field.....	56
Table 12	Pressure Function Calculated Results for Ethane and Propane	57
Table 13	Gas Composition with Different Specific Gravity.....	57
Table 14	Pressure Function Calculation for Formulated Gas Compositions	58

List of Figures

Figure 1 Gas Pressure Function Curve (Golan 1996), pp 135 32

Figure 2 A typical velocity profiles for laminar and turbulent flow 33

Figure 3 Tracer Distribution Pattern in a pipeline..... 33

Figure 4 Hydrate formation curve (Guo et al., 2005)..... 34

Figure 5 Amount of Asphaltene Precipitated as a function of Pressure (Guo et al., 2005) 34

Figure 6 A Typical Deposits layer in Pipeline 35

Figure 7 Amount of Scale Precipitated from mixture of Seawater and Formation water..... 35

Figure 8 Pressure Pulse Response for clean Pipe (solid line) and Pipe with Deposits (thin line)..... 36

Figure 9 Pipeline sections showing different deposits spread..... 36

Figure 10 Tracer Response at the Inlet and Outlet of a pipeline..... 37

Figure 11 Tracer Flow in Pipeline with Multiphase Fluid (Bjørnar 2005) 37

Figure 12 Tracer Response in Multiphase pipeline (Bjørnar 2005)..... 38

Figure 13 Pipeline with an undulating path (Bjørnar 2005)..... 38

Figure 14 HYSYS Simulation Model Window for the pressure function 38

Figure 15 Tracer Concentration Profile at Different Location for a uniform 8” (ID) Pipe..... 39

Figure 16 Tracer Concentration Profile at Different Locations with Different Pipe diameters 39

Figure 17 Tracer Pulses at the exit of the pipelines (100 km) with Different ID pipe..... 40

Figure 18 Effect of Pipe Diameter on Tracer Velocity Profile 40

Figure 19 A Tracer Concentration Profile at 20 km Downstream of Injection Point. 41

Figure 20 A Tracer Concentration Profile at 40 km Downstream of Injection Point. 41

Figure 21 Effect of Pipe Roughness on Tracer Dispersion for 8 inches ID Pipeline..... 42

Figure 22 Effect of Pipe Roughness on Tracer Dispersion for 6 inches ID Pipeline..... 42

Figure 23 Flow Meter Accuracy with Deposits Thickness 43

Figure 24 Pressure Function of Produced gases and Methane for different Fields..... 43

Figure 25 Pressure Function of Processed gases for different Fields 44

Figure 26 Comparison of Pressure Function of Produced and Processed Gas 44

Figure 27 Effect of Gas Gravity on Pressure Function 45

Figure 28 pressure Function for Methane, Ethane, and Propane 45

Figure 29 Effect of Temperature on Pressure function of gas with s.g = 0.6 46

Figure 30 Effect of Temperature on Pressure function of gas with s.g = 1.0 46

Nomenclature

A	Pipeline area, m ²
a	The speed of sound, m ² /s
A _d	Deposition area, m ²
C	Concentration, g/ml
C _s	The concentration of solid wax at the pipe wall, g/ml
d	Pipeline diameter, m
D _m	Molecular diffusion coefficient, m ² /s
D _o	Diffusion coefficient, m ² /s
D _x	Axial dispersion coefficient, m ² /s
K	Longitudinal dispersion coefficient, m ² /s
k _m	Constant,
k _w	Constant
L	Pipeline length, m
M	Mass of tracer injected, gram
m _s	Mass of the deposited wax due to shear dispersion of one mole of the liquid to the ideal gas state, gram
P _e	Peclet number, dimensionless
Q	Flow rate, m ³ /s
R	Ideal gas constant, j.mol ⁻¹ .k ⁻¹
r	Pipeline radius, m
R	Hydraulic radius, m
Re	Reynolds Number, dimensionless
T	Temperature, °C
t	Time, s
v	Average mean velocity, m/s
V _a , V _L	Molar volume of asphaltene and liquid oil phase respectively
v _o	Maximum velocity, m/s
Δu	Cohesive energy per mole (the energy change upon isothermal vaporization)
v _m	Molar volume
v _*	Shear of Friction velocity
W	Total wax mass deposited on the pipe wall.
x	Axial coordinate, m

dC/dr	Radial concentration gradient of the precipitated wax
dC/dT	Concentration gradient of the precipitated wax with respect to temperature
dT/dr	Radial temperature gradient.

Greek Letters

δ	Variance the measurement of spread of contaminates distribution
δ_s	The solubility parameter
δ_a, δ_L	Solubility parameter of asphaltene and liquid in oil respectively
ℓ	Characteristic length, m
f	Friction coefficient
ρ_w	Density of deposited wax, kg/m^3
μ	Fluid viscosity, Pa.s or cp
γ	Shear rate,
ϕ_a	Volume fraction of asphaltene in oil
α	Proportionality constant

1 Introduction

Technologies for estimating the thickness of deposits in pipelines have a significant impact in maintaining pipeline integrity. Deposits, especially wax precipitate on pipe wall through molecular diffusion, Brownian, settling, and shear dispersion mechanisms (Burger, et al., 1981). Deposition cause reduction of pipeline diameter and increase its wall roughness, thus increasing the frictional pressure and effectively reducing pipeline capacity. Thus it is essential to evaluate the amount of deposits in pipelines to enable a cleaning program to be effectively devised.

A good estimation of pipe deposits is required to ensure a satisfactory level of security and productivity. Among various technologies available, tracer technologies are widely used; it is applicable for either single or multiphase flow. The tracer technology is non-intrusive, and relies on the measurement of effective internal diameter of pipeline. Knowing the flow rate the effective internal diameter can be estimated by measuring the tracer pulse velocity through the pipeline.

Traditionally, estimation of tracer pulse velocity required estimation of longitudinal dispersion from tracer concentration profiles measured at least two sections downstream of the point of injection. However when the tracer concentration profiles of the stream is not available as it is applicable in this work, the predicted correlation for prediction of longitudinal dispersion coefficient is used to route the concentration profiles of tracer flow in the pipeline (Sushil et al., 2003).

Effect of pipeline roughness on tracer dispersion, sensitivity of flow meter accuracy on tracer technology accuracy, and application of the tracer technology to quantify the liquid accumulation in multiphase flow pipeline is also paid attention to.

Various deposits as applicable in oil and gas industry and available techniques for monitoring and estimation of pipelines deposits are reviewed. The parameters each technique depends on and major advantages and disadvantages of each application would be highlighted.

Analysis of pressure function of a given natural gas composition is important to predict productivity of gas wells using the rate pressure relation. From the literature the pressure

function is said to exhibit three distinct regions of behavior Figure 1. At high pressure the pressure function is said to be nearly constant. This assumption is investigated and presented in detail.

However the two unrelated topics covered in this thesis is due to their applications importance in oil and gas industry and also base on of my professor's interest on the two topics.

2 Taylor Dispersion in Pipeline

The term Taylor dispersion was coined as a tribute to G.I Taylor. Taylor in 1953 documented the mechanism by which a solute (brine) dispersed in a pipe. He described the dispersion or equivalently convection-diffusion phenomena to be governed by a combined effect of two physical phenomena, diffusion of solute across the pipe, and the differential longitudinal transport associated with the velocity shear over the cross-section of the pipe flow. The velocity shear causes the particles of solute located far from the pipeline walls to travel faster than particles located near the wall leading to rapid longitudinal spreading (Taylor 1953). A typical velocity profile developed in pipeline during the laminar and turbulent flows is shown in Figure 2.

On the other hand, diffusion acts to smear out the cross-stream (or lateral) gradients of solute concentration and, after a sufficient time the longitudinal distribution of the mean solute concentration will assume a Gaussian profile. Dispersion is one of the important phenomena known to depend fundamentally on flow conditions as well as on fluid and medium properties. Dispersion therefore acts against maintaining concentration difference (Svein and Jon 1992). Dispersion in pipeline can either be longitudinal or transversal, the former being dispersion along the pipe while the latter is dispersion or concentration variation across the pipe mean axis. For axial flow in pipeline, Taylor dispersion can be characterized by the mixing coefficient as shown in equation 2.1 below.

$$\delta^2 \alpha D_m t + t \left[\frac{r^2 v^2}{48 D_m} \right] \dots\dots\dots 2.1$$

Where, α is the proportionality constant, δ^2 a variance is the measure of spread of distribution, r (m) is the radius of the pipe, t (s) is the time, v (m/s) is the average mean velocity, and D_m (m^2/s) molecular diffusion coefficient

2.1 Dispersion Model

A dispersion model is used to describe the relationship between pipe flow and pipe hydraulic and geometries parameters. It considered the Fickian dispersion of matter described by a constitutive equation similar to the Fick's law of diffusion. The expression of the model results from a tracer mass balance injected at the feed of the system (pipeline). The model takes into account of two effects: convection, which represents the bulk flow, and dispersion,

which results from molecular and turbulent diffusion. There are two types of contribution to dispersion: Radial and Axial (Riquarts, 1981). The radial effect is negligible in comparison to axial effect when the aspect ratio L/D is greater than 4. The model is then called axial or longitudinal dispersion model. In this case, the concentration C (t, x) is a function of time and axial position in the pipeline, and it is described by the following expression.

$$\frac{\partial c}{\partial t} = D_x \frac{\partial^2 c}{\partial x^2} - v \frac{\partial c}{\partial x} \dots\dots\dots 2.2$$

Where C (g/ml) is the concentration of the tracer, v (m/s) the fluid velocity, D_x (m²/s) is the axial dispersion coefficient, x (m) the axial coordinate, t the time.

2.2 Mechanisms of Dispersion

Dispersion of a contaminant/tracer in a pipe takes places by molecular diffusion, turbulent diffusion and longitudinal shear flow dispersion, the latter being in the order of million times greater than the first two. However two major mechanisms; molecular diffusion and dispersion phenomena is highlighted below.

2.2.1 Molecular Diffusion

One of the fundamental processes for dispersion is molecular diffusion (Stalcup, 1983). Molecular diffusion is due to random kinetic motion of particles due to concentration gradient and resistance of solute to movement of solute molecules. Molecular diffusion is a mechanism that is discerns to be independent of fluid velocity. It is isotropic and acts very slowly. Molecular diffusion is more significant where the distance of interest is as small as possible, and at low velocity (pipe wall). This phenomenon is more applicable to describe the dispersion of fluid between fractures and rock matrix. However, velocity fields can be heterogeneous in pipe that neighboring streamlines may have vastly different velocities. As a result, diffusion from one streamline to another may have an impact on tracer transport/mixing especially near the pipe walls. Molecular diffusion phenomena is said to contribute to dispersion where the bulk flow approaches zero. This can be described by Fick's law;

$$\frac{dn}{dt} = -D_o A \frac{\partial c}{\partial x} \dots\dots\dots 2.3$$

Where $\frac{dn}{dt}$ is amount of chemical component (molecules), t (s) is time, A (m^2) is cross-section area D_o (m^2/s) is the diffusion coefficient, C (g/ml) the concentration and x (m) is the distance.

2.2.2 Taylor Dispersion

The spreading of concentration about mean displacement position, deviation of concentration from predicted by advection alone (spreading and dilution) is called Dispersion. This term is used primarily in association with the advection-dispersion equation. It accounts for diffusion-like “Fickian” spreading of mass during transport. The coefficient of dispersion is generally expressed as the combination of spreading in the direction of average linear velocity (longitudinal dispersion), and perpendicular to the direction of average linear velocity (transverse dispersion). Taylor dispersion acts primarily in the direction of flow. This is a fundamental difference between dispersion and molecular diffusion, as diffusion acts in all direction simultaneously (US EPA). Dispersion is also a function of velocity (mixing caused by flow velocities), whereas diffusion is independent of velocities variation of the flow medium.

2.3 Dispersion Regimes

The nature of dispersion in pipeline is controlled by the competition between molecular diffusion and convective dispersion. Different regimes of dispersion can be identified according to the Peclet number Pe , which is the ratio of between the typical time for diffusion ℓ^2/D_m and typical time for convection ℓ/v . Here v is the velocity of the carrier fluid, ℓ a characteristic length, and D_m the molecular diffusivity of the tracer. The Peclet number is thus defined as; $Pe = v \ell / D_m$. For small Peclet number regime, the transport of tracer in the pipe is dominated by molecular diffusion. So as $Pe \rightarrow 0$ the dispersion coefficient is simply proportional to molecular diffusivity D_m . However for a large Peclet number regime the transport is controlled by the convective dispersion. Here the tracer velocity is approximately equal to the carrier fluid velocity, and molecular diffusion plays little role (Hernan et al. 2000)

The tracer samples the disordered medium by following the velocity streamlines. The tracer particles is said to follow the direction of the velocity field, and taking steps of length ℓ and

duration of ℓ/v . Most transportation or flow through pipeline as obtain in oil and gas industry is being controlled by the convective dispersion. The tracer concentration profile of tracer in the pipe can be estimated as a function of Peclet number with the following equation.

$$C(t, x) = \sqrt{\frac{Pe}{4\pi t^*}} \exp\left[-\frac{(1-t^*)^2 Pe}{4t^*}\right] \dots\dots\dots 2.4$$

Where, $t^* = \frac{tv}{\ell}$

Pe = the Peclet Number (dimensionless), t (s) is the time, v (m/s) velocity of carrier fluid, ℓ (m) is the length of flow.

2.4 Dispersion Coefficient

Dispersion coefficient of is one of the crucial parameters that need to be estimated accurately in order to obtain a reliable results when dispersion model is being used to estimated the hydraulic and geometries properties of a pipeline. Dispersion in a pipe is cause by different phenomena such as: molecular diffusion, turbulent diffusion, and longitudinal shear flow dispersion. Among all these phenomena longitudinal shear dispersion is in the order of million times greater than the others. Therefore it is more paramount to estimate the longitudinal dispersion coefficient accurately. The Table 1 below shows the range of values for diffusion and dispersion coefficient for different process and direction of flow.

Table 1 Range of values for Diffusion and Dispersion Coefficients
(Source US EPA)

Process	Direction of flow	Typical Ranges in [m ² /s]
Molecular Diffusion	Vertical	10 ⁻⁸ to 10 ⁻⁹
	Lateral	10 ⁻⁸ to 10 ⁻⁹
	Longitudinal	10 ⁻⁸ to 10 ⁻⁹
Turbulent Diffusion	Vertical	10 ⁻⁶ to 10 ⁻²
	Lateral	10 ⁻² to 10 ²
	Longitudinal	10 ⁻² to 10 ²
Dispersion	Vertical	10 ⁻³ to 10 ⁻¹
	Lateral	10 ⁻² to 10 ⁰
	Longitudinal	10 ⁻¹ to 10 ⁴

2.4.1 Longitudinal Dispersion Coefficient

Longitudinal dispersion coefficient K can be computed analytically from a knowledge of the velocity distribution in a pipe which can be derived for either laminar or turbulent flow (Fisher et al. 1979). For laminar flow the following equation which relate dispersion to both diffusion and convection results.

$$K = \frac{d^2 v_o^2}{768D} \dots\dots\dots 2.5$$

Where K is the Dispersion Coefficient (m^2/s) d (m) is the pipe diameter, v_o (m^2/s) is the maximum velocity at the pipe center, v (m/s) is the mean velocity in the pipe and D_m (m^2/s) is the molecular diffusion coefficient of the solute.

For turbulent flow as it is more applicable to most of the flows in oil and gas industry the longitudinal dispersion coefficient can be estimated using the available concentration profiles of a tracer’s flow in the pipe measured at least in two sections of the pipe. If the tracer experiments are not available as it applicable in this thesis, the predicted correlations for the estimation of longitudinal dispersion coefficient is used, hence the concentration profiles of the tracer flow in the pipe can be generated. A typical tracer concentration developed in pipeline is shown in Figure 3. The predicted correlations by different authors which related the longitudinal dispersion coefficient (K), hydraulic radius of the pipe (R), mean flow velocity (v), and the shear or friction velocity (v_*) are expressed below.

The equation proposed by Fisher et al. (1979) is;

$$K = 5.05dv_* \dots\dots\dots 2.6$$

The equation Proposed by Magazine et al. (1988) is;

$$K = 75.86Ru \left(0.4 \frac{u}{v_*} \right) \dots\dots\dots 2.7$$

Where, R (m) is the Pipe hydraulic Radius, u (m/s) is velocity.

The equation proposed by Liu (1977) may be written as;

$$K = 0.18 \left(\frac{v_*^{0.5} Q^2}{u^{1.5} R^3} \right) \dots\dots\dots 2.8$$

Where v_* is the shear (or friction) velocity at the periphery of the pipe, the friction velocity is related to the friction factor as expressed in equation 2.9.

$$v_* = \sqrt{\frac{f}{8}}v \dots\dots\dots 2.9$$

Where the friction coefficient f is a function of Reynolds Number Re . the Reynolds Dimensionless number is introduced to account for the effect of fluid rheologies on the dispersion of molecules in pipes. For a smooth pipe the following approximation can be used to estimate friction coefficient explicitly within the range $4000 < Re < 10^5$ (Blasius, 1911)

$$f = 0.316Re^{-\frac{1}{4}} \dots\dots\dots 2.10$$

Longitudinal dispersion increases with greater wall friction and for turbulent flow the friction factor is expressed by Halaand, 1983 and given below

$$\sqrt{\frac{1}{f}} = -\frac{1.8}{n} \log \left[\left(\frac{6.9}{Re} \right)^n + \left(\frac{k}{3.75d} \right)^{1.11n} \right] \dots\dots\dots 2.11$$

$n = 3$ for gas

$n = 1$ for Liquid.

Source (Gudmundsson, 2005)

Where k (mm) is the pipe roughness, d (m) is the pipe diameter, and Re the Reynolds Number

which is defined as $Re = \frac{\rho vd}{\mu} \dots\dots\dots 2.12$

Where ρ (kg/m^3) is the fluid density, μ (pa.s) is the fluid viscosity, and v (m/s) is the fluid mean velocity in the pipe

However once the longitudinal dispersion coefficient is estimated the concentration variation along the pipe length is expressed as proposed by Taylor (1954);

$$C(x,t) = \frac{M}{A\sqrt{4K\pi t}} \exp\left(-\frac{(x-vt)^2}{4Kt}\right) \dots\dots\dots 2.13$$

Where $C(x,t)$ is the concentration of the tracer downstream of the injection point (g/ml), M is the mass of the tracer injected (gram), t (s) is the time, v (m/s) is the mean flow velocity, x (m) distance downstream of the injection point, and K is the longitudinal dispersion coefficient (m^2/s).

3.0 Deposit Formations in Pipeline

There are numerous deposits which are encountered when transporting oil and gas through pipelines. The major deposits found in pipelines are as follow: the Wax, Hydrate, Asphaltene, and Scales.

3.1 Wax Depositions

Crude oil is a complex mixture of hydrocarbons which consist of aromatics, paraffins, naphthenics, resins, asphaltenes, mercaptans, etc. When the temperature of crude oil is reduced the heavy components of the oil like paraffins/wax (C_{18} - C_{60}), will precipitate and deposit on the pipe wall. The pipe internal diameter will reduce due to wax deposition. Wax solubility in aromatic and naphthenics is low, and it decreases drastically with decreasing temperature. Thus it is easy for wax to precipitate at low temperature. The highest temperature below which the paraffins start to precipitate as crystals is defined as crude cloud point or wax appearance temperature. Since light oil stabilizes the paraffins molecules (Meray, et al, 1993), the cloud point of live oil (oil with solution gas) with pressure below the bubble point is usually lower than the cloud point of the dead oil (oil without solution gas).

Extensive research has been conducted to try to understand and model the wax deposition process which is a complex problem involving fluid dynamics, mass and heat transfers, and thermodynamics (Burger et al., 1981). It is widely accepted that molecular diffusion of paraffin is one of the dominant deposition mechanisms. Other proposed mechanisms are: Brownian motion, gravity settling, and shear dispersion.

3.1.1 Molecular Diffusion

When waxy crude is flowing in pipeline, the temperature at the center of the pipeline is the hottest while the temperature at the wall is the coldest, resulting in a radial temperature profile. Since the wax solubility in oil is a decreasing function of temperature, when the temperature is lower than the cloud point, wax crystals will come out of solution. Thus the radial temperature gradient will produce a concentration gradient of wax in oil with the wax concentration in the oil lowest close to the pipe wall. The concentration gradient would result in mass transfer of wax from the center of the pipe to the pipe wall by molecular diffusion. (Hsu et al. 1995). Wax mass transfer can be described by the Fick's law as:

$$\frac{dw}{dt} = \rho_w A D_m \frac{dC}{dr} = \rho_w A \left(\frac{k_m}{\mu} \right) \frac{dC}{dT} \frac{dT}{dr} \dots\dots\dots 3.1$$

Where, W = total wax mass deposited on the pipe wall.
 t = time, k_m = constant, ρ_w = density of deposited wax
 μ = fluid viscosity
 D_m = Molecular diffusion coefficient of precipitated wax
 A = Pipe wall area available for wax deposition
 dC/dr = Radial concentration gradient of the precipitated wax
 dC/dT = Concentration gradient of the precipitated wax with respect to temperature
 dT/dr = Radial temperature gradient.

3.1.2 Other Proposed Mechanisms

Wax deposition is believed to be enhanced by Brownian motion. Once the temperature is below the cloud point, wax crystals will precipitate out of solution and be suspended in the oil. The suspended wax crystals will collide with each other and with oil molecules by Brownian motion. Because of wax concentration gradient, it is possible that the net effect of Brownian motions is to transport the crystals in the direction of decreasing concentration. It is suggested that deposition can occur due to Brownian diffusion of wax crystals.

Gravity settling as one of the possible mechanisms is based upon the argument that wax crystals tend to be denser than oil and would settle in a gravity field and deposit on the bottom of the pipeline. But experiments with horizontal and vertical flows showed that there was no difference in the amount of wax deposited for the two configurations. Thus, it is not yet clear how significant the gravity would affect wax deposits.

Burger et al. (1981) reported possible wax deposition by shear dispersion. He claimed that shear dispersion played a role in wax deposition mainly in laminar flow and proposed the following equation for the deposition rate.

$$\frac{dm_s}{dt} = k_w C_s A_d \gamma \dots\dots\dots 3.2$$

Where, m_s = mass of the deposited wax due to shear dispersion
 k_w = Constant

C_s = the concentration of solid wax at the pipe wall

A_d = deposition area

γ = shear rate

3.2 Hydrate Depositions

Gas hydrates are crystalline compounds that occur when small gas molecules (methane, ethane, propane, CO_2 , H_2S) contact with water at certain temperature and pressure. Hydrates are formed when the gas molecules get into the hydrogen-bonded water cages. It is believed that the formation of the hydrates nuclei usually initiated at the gas water interface. The crystals then grow by surface sorption of gas and water molecules (Makogon, 1997). Hydrates can form at temperature well above 32 °F (0 °C) in pressurized systems. Commonly found hydrates crystals structures identified are called structure I, II, and H. The properties of structures I and II are well defined while that of structure H are relatively new. Gas hydrates are like a solid, and their physical properties are similar with that of ice (Sloan, 1998). When hydrates form in the pipeline it reduce it diameter and the capacity thus reducing production throughput of the pipe. Hydrate plugs can also blocked the pipeline completely.

Sub-sea pipeline design and operations can be well guided by the hydrates curve. A typical hydrates curve is shown in Figure 4. On the left side of the curve is the hydrate formation region, when pressure and temperature are in this region, hydrate is likely to form in pipeline. On the right side of the curve is the non-hydrate formation zone. The hydrate formation curve is commonly impacted by the fluid composition, water composition, and salinity. The curve shows that with the initial system in the non-hydrate region, if the system pressure is increased while the temperature is kept constant, hydrate would eventually form. The same applied by reducing the system temperature at constant system pressure.

3.3 Asphaltene Depositions

Asphaltenes are defined as the compounds in oil that are insoluble in n-pentane or n-hexane, but soluble in toluene or benzene. That is Asphaltenes solids would precipitate when excess n-pentane or n-hexane is added to the crude oil. Asphaltene solids are dark brown or black and will not melt unlike waxes. But like waxes, with changes in pressure and temperature and composition, asphaltenes tends to flocculate and deposit in pipeline. Mixing two oil streams can also induce asphaltene precipitation (Wang et al. 2003).

The saturation of asphaltenes in crude oil is a key parameter to determine whether or not asphaltene would deposit in pipeline during transportation. If asphaltenes are under-saturated in crude oil no precipitation will occur since asphaltenes are stable at under-saturated condition. But asphaltenes would precipitate if they are highly super-saturated. The saturation of asphaltenes can change from under-saturated to super-saturated if the pressure, temperature and composition change. Thus during oil and gas production and transportation asphaltenes precipitation inside the pipeline is a potential risk.

A parameter that is closely related to asphaltenes stability is solubility. Solubility parameter is a function of temperature (Barton, 1991). Increasing temperature tends to decrease the asphaltene solubility parameter. Therefore solubility parameter of oil and asphaltenes are the key input data for most of the thermodynamic models for asphaltene phase behavior. The solubility parameter is defined as:

$$\delta_s^2 = \frac{\Delta u^v}{v_m} \dots\dots\dots 3.3$$

Where, δ_s = the solubility parameter

Δu = cohesive energy per mole (the energy change upon isothermal vaporization of one mole of the liquid to the ideal gas state)

v_m = molar volume

The pressure effect on asphaltene solubility depends upon the pressure being above the bubble point or below the bubble point (Hirschberg et al. 1984). The pressure dependence of asphaltene solubility in crude oil is shown in Figure 5. When the pressure is above the bubble point, the fluid composition is constant, but with decreasing pressure, the density of crude decreases due to oil expansion, and so does asphaltene solubility. The asphaltene solubility reduces to a minimum when pressure is approaching the bubble point. Below the bubble point, gases start to come out from live oil and the oil density increases. The asphaltene solubility also increases with decreasing pressure. The loss of light ends improves the asphaltene stability in crude oil. Assuming the asphaltene and crude oil are in equilibrium (no asphaltene precipitation), the maximum volume fraction of asphaltenes soluble in the crude is given by the Flory-Huggins theory (Hirschberg et al., 1984) as follow:

$$(\phi_a)_{\max} = \exp\left\{\frac{V_a}{V_L}\left[1 - \frac{V_L}{V_a} - \frac{V_L}{RT}(\delta_a - \delta_L)^2\right]\right\} \dots\dots\dots 3.4$$

Where, ϕ_a = volume fraction of asphaltene in oil

V_a, V_L = molar volume of asphaltene and liquid oil phase respectively

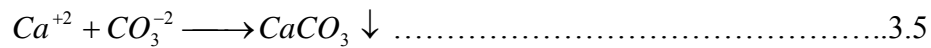
δ_a, δ_L = solubility parameter of asphaltene and liquid oil respectively

T = Temperature

R = ideal gas constant

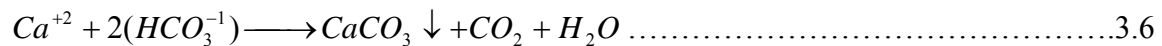
3.4 Scale Depositions

Scale is a potential precipitates from water unlike waxes and asphaltenes which precipitates from crude oil. The primary effect of scale growth in pipeline is to lower the production rate by increasing the surface roughness of the pipe and reducing the flow area. The driving force therefore goes up and the production goes down. The most common scales occurring in oil and gas industry are calcium carbonate, barium sulfate, strontium sulfate and calcium sulfate. Calcium carbonate ($CaCO_3$) is also called calcite scale. Calcite scale is formed when the calcium ion is combined with the carbonate ion (Guo et al. 2005)



Where, Ca^{+2} is Calcium ion and CO_3^{-2} is the Carbonate ion.

Calcium carbonate is a solid and can potentially precipitate from solution to form scale. Similarly, when the calcium ion is combined with the bicarbonate ion, calcium carbonate will also be formed.



Where, HCO_3^{-1} is the bicarbonate ion.

Barium sulfate is formed when the barium ion is combined with the sulfate ion:



Where, Ba^{+2} is the barium ion, and SO_3^{-2} is the sulfate ion.

Figure 6 show a Common scaling scenarios encountered in hydrocarbon productions and transportations. There are many factors which cause scale deposits in pipelines, a few of the factors are discussed below;

3.4.1 Incompatible Mixing

Sea water used for secondary and enhanced recovery water flooding operations and formation water often mix together near the well bore matrix to produce another fluid composition with combined ions concentration that are above the solubility limits for sulfate minerals. The mixture can also occur in pipeline thus enhanced scale deposit. Figure 7 shows the amount of scale that precipitates from different mixture of sea water and formation water.

3.4.2 Auto-scaling

Fluid experiences changes in temperature and pressure as it flow through pipeline or in the reservoir. If such changes take the fluid composition beyond the solubility limit for a mineral, it will precipitate as scale. Sulfate and carbonate scales can precipitate as a result of pressure changes within the well bore matrix, along tubing, pipeline and into surface facilities as long as the produced water continuously changes in pressure and temperature.

4 Pipeline Deposits Evaluation Techniques

The best technique to be adopted for the removal of deposit in pipeline depends on knowing the amount of deposits present. There are many techniques used in oil and gas industry to evaluate the amount of deposits in pipelines. A few out of many applications available will be highlighted in this thesis work. The main focus will be base on the basic parameters each technique depend on and their possible advantages and disadvantages.

4.1 Pressure Pulse Techniques

The pressure pulse technology is one of the new technologies used to estimate/monitor deposits in pipeline (Gudmundsson and Celius, 2005). The technology is base on the water hammer equation, the pipeline pressure drop equation, and the equation for speed of sound in single phase fluids and in multiphase mixtures. The technology can therefore applicable in detection of deposits in pipes with flowing liquids, gases and multiphase mixtures. Measurement of deposits is achieved by generating a pressure pulse in the pipeline by activating a valve in a multiphase pipeline. The pressure pulse propagated both upstream and downstream of the valve. The magnitude of the pulse is governed by the water- hammer equation.

$$\Delta P_a = \rho u a \dots\dots\dots 3.8$$

Where, ρ (kg/m³) is the fluid density, u (m/s) is the fluid velocity, and a (m/s) is the speed of sound in the fluid.

Another important parameter which pressure pulse technology base on is the line packing. This is a phenomenon which occurs due to manifestation/released of pressure loss due to pipe wall friction as the flow is brought to rest. The gradual pressure increase (pressure gradient) after the water hammer is the line packing and the frictional pressure drop in pipes is governed by the following equation.

$$\Delta P_f = \left(\frac{f}{2}\right)\left(\frac{\Delta L}{d}\right)\rho u^2 \dots\dots\dots 3.9$$

Where, f (dimensionless) is the friction factor, ρ (kg/m³) fluid density, ΔL (m) pipe length, d (m) the pipe diameter, and u (m/s) is the fluid velocity.

The water- hammer and line packing pressure pulse shown in Figure 8 depicts the clean pipeline flow and pipeline with deposits. Estimation of the deposits thickness is attained by

analysis of the line packing pressure zone. Knowing the mass flow rate, the thickness of the deposited material can readily be calculated from the water-hammer equation (equation 3.8), the measured water-hammer pressure increase is proportional to the fluid velocity.

$$u = \frac{\Delta P_a}{\rho a} \dots\dots\dots 3.10$$

The squared of pipe diameter is related with the mass flow rate and fluid velocity as follow;

$$d^2 = \frac{4m}{\pi u} \dots\dots\dots 3.11$$

Where, m (kg/s) is the mass flow rate.

The reduction in flow diameter due to deposits in the pipeline as compared with the clean pipeline shows the thickness of deposits present in the pipeline, and the amount can be estimated by multiply the reduced flow area with the pipeline length.

4.2 Pressure Drop Technology

The basis of the pressure drop technology is that pipeline deposition reduces the hydraulic diameter of the pipeline flow and therefore increases the frictional pressure drop over the pipeline section. This technology does not require depressurization and restart of pipeline. Unfortunately, pressure drop technology is not accurate for deposit evaluation, especially in the multiphase flow case, due to the extremely complicated and characteristics of the pressure drop which make changes difficult to interpret. As shown in Figure 9, Alberto, 2006 observation shows that for a steady-state measurement along 5 km pipeline with distributed deposit thickness of 0.5 inches, and 73 m³ volumes induced the same pressure drop with thin 90% obstruction deposit of 0.5 m³ volume.

4.3 Pigging Technology

Traditionally, a mechanical device called a pig has been used for deposit evaluation. The deposit thickness is obtained by passing the pig through a pipeline and measuring the volume of the deposit removed. Moreover, only about 25-30% of the current pipelines are capable of using pigs. The rest of pipelines lack pig launchers and catchers, or contain obstructions that prevent pig use. The cost of pig launchers and receivers in terms of downtime and maintenance can be immense (Gelman et al. 2003). Consequently, there is real need for a more effective method for detecting and measurement of pipeline deposition.

4.4 Thermal Technology

The thermal heat transfer technology is based on measurement of thermal flux, which depends on deposit thickness. This technology can give acceptable accuracy if the film heat transfer coefficients on the inside and outside of the pipeline walls are calculated properly. This technology however, is not sufficiently accurate for deposit detection, due to thermal expansion load and stresses in pipelines (Gelman et al 2003). It is especially unsuitable for multiphase flow because the multiphase heat transfer coefficients inside the pipeline are subjected to large uncertainty.

4.5 Spool Piece Technology

Spool piece technology involves removing of a pipeline section and determining the deposit thickness by measuring the weight or volume of deposits removed from the section. This simple technology allows visual examination of the deposits (Gelman et al. 2003). This approach requires the dismantling of the section of pipeline and this interferes with the production schedules. This disadvantage is more complex for high pressure pipes; these pipelines must be depressurized first, and this cause a change in phase equilibrium.

5 Tracer Technology

Tracer technology works by injecting small mass/volume of tracers that are selective with oil, water or gas phases. These tracers could be dye tracers, but could also be other types of materials e.g. fluorescent or radioactive tracers. By injecting these tracers at known rates, and by analyzing a sample of the single or multiphase flow sufficiently far downstream of the injection point, the individual phase flow rates and velocity of fluid at a particular location along the flow path can be determined by measuring the dilution and the tracer pulse generated.

The uncertainty of the tracer technique will depend on the composition, flow regime and accuracy of the fiscal flow meter. The expected uncertainty should be established for each specific application. The use of this technique therefore requires that suitable points for injection and sampling be included in the installation.

5.1 Tracer Flow Concentration Profiles

The concentration distribution of the tracer between the upstream section (injection point) and the downstream sections (observation point) is used to measure the flow velocity in the pipeline. The concentration profile at the upstream section can be assumed to consist of a series of pulse concentrations of infinitesimal duration. The concentration profile at the downstream section is then the sum of the responses due to these pulse concentrations at the upstream section.

The narrow pulse of tracer injected at the upstream section is observed to widen, and nearly symmetrically distributed about the point of maximum concentration as the tracer move further downstream, in spite of the fact that the distribution of the velocity over the section which give rise to this dispersion is highly unsymmetrical. The phenomenon observed downstream of the injection section Figure 10 is due to molecular diffusion and dispersion which act on the tracer molecules as it flow through the pipeline. The molecular diffusion or dispersion in return depends on the hydraulic geometry of the pipeline and the flow regime. The tracer pulse can be generated using proposed equation by Taylor (1954) as stated in equation 2.11.

5.2 Tracer Transit Time

One important parameter needed to measure the amount of deposits in pipelines involves the estimation of tracer residence time distribution (RTD) as it pass through the test sections. Mean residence time can be obtained by recording the time at the upstream section where the tracer pulse is first observed and at the interest locations downstream section where the tracer pulse is observed again. This procedure can be repeated until the total residence time of tracer in the pipeline is recorded.

5.3 Tracer Mean Velocity

The downstream concentration profile of tracer flow in pipeline is a function of Velocity profiles developed due to friction mechanism. Therefore if downstream concentration in the entire cross section flowing past the detection point could be measured, the mean velocity of the tracer correspond to a travel time point, t , on the detection profile, at which the concentration of tracer is one-half of the maximum concentration can be estimated with the following simple relationship (Bischoff et al. 1963)

$$u = \frac{L}{t} \dots\dots\dots 5.1$$

Where L (m) is the injection to detection distance, t (s) is the time of flight of tracer.

5.4 Effect of pipe Roughness on Tracer Flow

The deposits in pipelines, apart from reducing the hydraulic diameter of pipelines it also increases its roughness thus increase the pipe wall friction. The longitudinal dispersion coefficient is said to increase with pipe roughness. The degree of friction during the flow of tracer molecules in a carrier fluid flowing through a pipeline is expressed using Halaand friction equation as shown in equation 2.9.

From Halaand equation the pipe roughness k , was varied to obtain different friction factor. The new friction factor is then used to calculate another shear velocity and the corresponding longitudinal dispersion coefficient which is then substitute into the tracer concentration response equation. It was found that the pipe roughness increases the mixing of tracer molecules in a carrier fluid. A plot of Concentration response is plotted against the pipeline distance.

5.5 Flow Rate Measurement Sensitivity on Tracer Testing

The performance of real-time deposits evaluation in pipelines systems using the tracer technology is limited primarily by the accuracy of the instrumentation installed on the line especially the fiscal flow meter. To estimate the minimum amount of deposit that can be detected for different pipelines diameters, it is important to understand the effect of fiscal flow meter uncertainty on the model. Deposits thickness causes reduction in pipeline area relative to its area with no deposits. The % changes in the area due to deposit thickness should be detected by the flow meter for accurate deposits evaluation. Table 3 shows the summary of available flow meters and the accuracy for each. As applicable in oil and gas industry a flow meter with 95% accuracy is common. Effect of % flow measurement meter accuracy on the minimum deposits thickness that can be detected for different internal diameters pipelines is presented. Detail calculations are expressed in appendix B.

5.6 Estimation of Deposits in Pipeline

Evaluation of deposit in pipelines using tracer technology involves accurate measurement of tracer pulse velocity through the entire length of the pipeline. The exact time the tracer pulse passed a known position at the entrance of the pipeline and the time of eventual arrival of the pulse at the exit is measured. A simple measurement of tracer flow velocity is obtained by dividing the time of flight of the pulse by the total distance traveled.

The fiscally metered flow rate during the tracer test is then compared to the measured tracer pulse velocity, thus allowing the effective average internal diameter of the pipeline to be calculated. Any reduction from the internal diameter schedule of the pipeline will be due to deposit within the pipeline. The flow is assumed to be full bore and turbulent during the measurement period. The technology can be used to estimate deposits within the pipe at any location of interest along the pipe.

5.7 Estimation of Liquid Loading in Pipeline

Pressure and temperature variation of gas condensate flows in a pipeline may cause partial gas condensation. Gas condensate pipeline will always operate in the single phase mode as long as its operational region or pressure-temperature path lies outside the phase envelope to the right of the dew-point curve. However in many cases, some liquid is formed somewhere along

the pipeline as shown in figures 11 and 12. Pipelines in undulating terrains tend to accumulate more liquid than pipeline in flat terrains. A typical pipeline with an undulating part is shown in Figure 13.

Optimal operation of pipeline requires estimation of liquid accumulation (Condensate and water/MEG). One of the direct, non-intrusive measurements, new techniques discovered so far is the tracer technology. This technology involves injection of tracer at the inlet of the pipeline, sampling of the outlet tracer concentrations of both phase and measurement of tracer residence time. For accurate measurement, the flow conditions are assumed to be steady-state (at equilibrium), full bore flows and no production disturbance. Also the fluid composition, pressure and temperature profiles, liquid holdup distribution (using OLGA-simulation), thermodynamic properties of the fluid (PVTsim), measurement of outlet liquid flow, and tracer transport time need to be estimated. The choice of tracers employed also plays a major role in order to obtain maximum accuracy. The use of a tracer with constant concentration, high solubility in the liquid phase with small amount in the gas phase along the pipeline should be employed.

Accumulated liquid in pipeline can be calculated by estimation of outlet liquid flow from the tracer response. This procedure is called the tracer dilution mass flow measurement method. The total injected tracer flow at the inlet is measured (Bq/s), and at equilibrium the same total tracer flow is expected to appear at the outlet. The tracer concentrations at downstream sampling points are directly dependent on the flow rate of each phase (the higher the flow the lower the tracer concentration). Subtracting the tracer flow in the gas phase, the tracer flow in the liquid at the outlet (I_{ol}) can be estimated. By measured the liquid tracer concentration (C_L) at the outlet (Bq/ml), then the outlet liquid flow can be estimated (I_{ol}/C_L), hence the liquid accumulated (Bjørnar 2006). The following equation summarizes how the liquid accumulated in a pipeline can be estimated.

$$L_{Acc} = q_i - q_{go} - q_{Lo} \dots\dots\dots 5.2$$

Where,

$$q = \frac{I_{ol}}{C_i} = \left(\frac{Bq}{s} * \frac{ml}{Bq} \right) = \frac{ml}{s} \dots\dots\dots 5.3$$

Where, L_{Acc} is the liquid accumulated in the pipeline (ml/s), q_i the total flow at the inlet (ml/s), q_{go} Is the outlet gas flow (ml/s), q_{Lo} the outlet liquid flow (ml/s).

6.0 Pressure Function for Gas Wells

6.1 Gas Pressure Function at High Temperature and Pressure

Pressure functions for natural gas is an important phenomenon which shows the relationship or behavior of natural gas properties such as viscosity and compressibility factor with pressure and temperature. This need to be determined and analyzed in order to predicts and optimizes gas well productivity and performance. Pressure functions help to determine the temperature and pressure range at which natural gas is available and this help to determine which pressure rate equations suitable for prediction of gas well inflow performance and the productivity index.

The pressure function behavior of natural gases at high temperature and pressure as found in the North Sea was investigated. The PVT properties (molecular weight, viscosity, compressibility factor) of gas compositions from different fields were analyzed using HYSYS process simulator. The temperature was kept at about 150 °C, while the Pressure is adjusted from 0 – 350 bars.

6.2 Effect of Fluid Properties on Pressure Functions.

The natural gas properties depend on its composition. Different gas compositions from produced and processed gas were analyzed to see the effect of gas properties (molecular weight and specific gravity) on gas pressure function. To investigate the effect of gravity on gas Pressure function, different gas compositions was formulated by adjusting the composition in order to obtain composition with specific gravity ranges from 0.6 – 1.0.

The formulated gas compositions using HYSYS process simulator was obtained by taken a sample of natural gas composition from a text (Gudmundsson 2006), an excel sheet created within the HYSYS was used to adjust the gas compositional fractions till a gas with required specific gravity was obtained. The values obtained were then simulated to generate the pressure functions parameters for each gas composition obtained. The HYSYS process simulated window is shown in Figure 14

6.3 Effect of Temperature on Pressure Functions

The effect of temperature on pressure functions of natural gas was investigated. Temperature for different gas compositions was varied to show the effect of temperature on gas viscosity

and compressibility factor. The pressure functions values generated at temperature of 50, 100 150 °C is then plotted to see the effect of temperature. The gas specific gravity in this case is kept constant.

7 Discussions of Results

The primary aim of this thesis work was to investigate the use of tracer technology for testing of pipeline with deposits. The analysis was based on Taylor dispersion of fluid in a pipe. The major parameter which dispersion depends on and flow rate measurement sensitivity on the accuracy of the technology were investigated and analyzed. Application of tracer technology in multiphase flow pipeline to measure liquid accumulation in pipeline was also highlighted.

Another phenomenon investigated in this thesis is the analysis of gas pressure function. The analysis was based on calculation of PVT properties (M_g , μ_g , γ_g , Z_g) of different gas compositions using HYSYS process simulator. The effect of gas specific gravity on pressure function curve behavior was investigated and analyzed.

7.1 Effective Internal Pipeline Diameter

Measurement of deposits in pipeline using tracer technology depends on accurate measurement of effective internal diameter of a given pipeline. Figure 15 shows the tracer pulse response flowing through a pipeline with uniform internal diameter of 8 inches and 100 km long. The pulse generated was observed at different location downstream of injection point. The time of flight/residence time between two successive equal distances is the same which signify a uniform tracer velocity response. The concentration profile shows a wider and decrease in maximum concentration downstream of the flow, this is attributed to increase in mixing due to longitudinal dispersion increase down the stream.

The effect of reduction in pipeline internal diameter was analyzed as shown in Figure 16. It was observed that as the internal diameter decreases, the tracer pulse time of flight/residence time decreases. Figure 17 also shows the tracer pulse residence time at the exit of different pipeline with different internal diameter (6 – 8 inches). The pulse residence time at the exit of the pipe with 6 inches internal diameter was observed to be earlier than that of pipeline with internal diameters of 7 and 8 inches. Figures 18 and 19 shows magnified tracer response downstream of injection point at 20 km and 40 km respectively.

Figure 20 therefore shows an inverse proportional relationship between the tracer velocity and the internal diameter of the pipeline. Therefore deposits in pipeline were observed to be proportional to tracer residence time and inversely proportional to tracer velocity in the pipeline.

7.2 Effect of Pipeline Roughness on Tracer Flow

One of the parameters dispersion in pipe flow depends on is the pipe roughness. Deposits in pipeline increase its roughness and in return increase the longitudinal dispersion coefficient. Figures 21 and 22 show the effect of pipe roughness on tracer dispersion for pipe with 8 and 6 inches internal diameters respectively, it was observed that the tracer pulse concentration decreases with pipe roughness. However the pipe roughness may drop the tracer maximum concentration below detectable limits.

7.3 Sensitivity of Tracer Testing on Flow Rate Measurement

The accuracy of tracer testing of pipeline with deposits depends on the fiscal flow rate measurement accuracy. Deposit thickness reduced the effective internal diameter of the pipeline thus cause a decrease in it area. Figure 23 shows the relationship between the deposit thickness and the % change in area for pipeline with different internal diameters. The deposit thickness detected increases with pipeline initial internal diameter for a given flow meter accuracy. For 5% flow meter accuracy the minimum deposits thickness for 8, 7, and 6 inches initial internal pipeline diameters are 2 mm, 2.2mm and 2.3 mm respectively. The higher the accuracy of the flow meter the higher the minimum deposits thickness that can be detected in a pipeline. A flow meter with 0.25% flow accuracy such as turbine as shown in Table 3 could detect deposit thickness less than 1 mm.

7.4 Effect of Gas Specific Gravity on Pressure Function

The pressure function of produced and processed gases from different fields with different composition and methane gas was plotted as shown in Figure 24 and 25 respectively. The pressure function curve generated shows a linear relationship that $1/\mu_g Z$ is essentially constant at low pressure range (usually less than 110bars) for gas composition with specific gravity in the range of 0.554 – 0.67. As the pressure increases, that is at pressure range between 110 – 275 bars the pressure function shows a distinct curvature.

Figure 26 shows the comparison of pressure function of produced and processed gas, the pressure function for gas composition with specific gravity in the range of 0.58- 0.67 shows similar behavior as stated above. While the gas composition with specific gravity greater than 1 mm (Draugen gas composition) shows different behavior. The pressure function curve

shows a distinct curve even at low pressure, but flattens out as the pressure increases. This behavior is similar to the pressure function curve for ethane and propane with specific gravity of 1.038 and 1.53 respectively as shown in Figure 27.

Figure 28 shows the effect of gas gravity on the gas pressure function. It was observed that as the specific gravity increases the pressure function at high pressure (pressure above 275 bars) started to move downward and flatten out which indicate that the pressure function ($P/\mu_g Z$) is constant at high pressure.

7.5 Effect of temperature on Pressure Functions

Figures 29 and 30 show the effect of temperature on natural gas pressure functions curve. The pressure and temperature show similar effect on the curves behaviors, except that the temperature shift the functions upwards at low pressure range, while at high pressure the pressure functions shift downward as the temperature decreases.

8.0 Conclusions

Based on the literature reviewed and the calculated results the following conclusions are drawn, however the conclusions are presented in two parts. First conclusion is related to the tracer technology and the second one is the pressure functions conclusion.

Tracer Technology Conclusions

1. The Tracer Technology is based on Taylor dispersion model and can readily be used to estimate the amount of deposits and liquid accumulation for both single and multiphase flows in pipelines.
2. Measurement of deposit in pipelines using tracer technology depends on estimation of effective internal diameter of a given pipeline. The effective internal diameter is obtained by comparing the flow rate with the measured tracer pulse velocity through the pipelines.
3. The accuracy of tracer technology for quantifying deposits in pipeline depends on accurate flow rate measurement.
4. As the pipeline roughness increases, the Tracer maximum concentration decreases, the dispersion increases and the tracer pulse widens as the maximum concentration lowers.

Pressure Functions Conclusions

1. The pressure functions curve for gas composition with specific gravity in the range of 0.554 – 0.67 is linear at low pressure (< 100 bars) and non-linear at high pressure greater than 100 bars.
2. The pressure functions for gas composition with specific gravity greater than 1 shows a distinct curve at low pressure, but constant at high pressure.
3. The pressure functions in linear and shift upward as the temperature decreases at low pressure range and at high pressure the curve is constant and tends to shift downwards as the temperature decreases.

Reference:

Ajay, A et al., 2000 “Taylor dispersion, Final project, Department of Bioengineering university of Pennsylvania, the link is

<http://www.seas.upenn.edu/courses/belab/LabProjects/2000/be310s00t2.doc>

Barton, A. F. M. 1991, CRC Handbook on Solubility Parameters and Other Cohesive parameters, 2nd Edition CRC press, Boca Raton.

Bischoff, K. B. et al. 1963, ”Theory of Tracer Flow”, SPE 718, pp 1- 7.

Bjørnar, H. K., 2006 Field experience on gas condensate flow measurements versus simulation, weekly multiphase guest lecture at IPT NTNU, Trondheim, Norway, link

<http://www.ivt.ntnu.no/ept/fag/tep4250/>

Burger, E. D. et al. 1981, ”Studies of Wax Deposition in the Trans-Alaska Pipeline”, Journal of Petroleum Technology

Donald, L. K., Robert, L. L, 1990 “Natural gas engineering production and storage”, Chemical engineering series, McGraw-Hill international Edition, Pp 197 – 227

Engineers Edge: http://www.engineersedge.com/fluid_flow/flow_velocity_profiles.htm

Fisher, H.B., List, E.J., Koh, R.C.Y., Imberger, J. and Brook, N.H. “Mixing in Inland and Coastal Waters,” 1979 Academic press, New York, pp 483.

Gelman, L. et al. 2003 “Vibro-acoustic Deposit Detection in Pipelines”, Insight Vol 45 No 7 July 2003; <http://www.atypon-link.com/BINT/doi/abs/10.1784/insi.45.7.466.54456>

Golan, M. and Curtis, H. W., 1996 “Well Performance”, Tapir Edition, Norway

Gudmundsson, J. S, 2005 ”Trykktap, Temperatur og Hydrat”, TPG 4140 Naturgass lecture Note .

Gudmundsson, J. S. 2006 “Processing of Petroleum”, Lecture note 2006

<http://www.ipt.ntnu.no/~jsg/undervisning/prosessering/TPG4135.html>

Gudmundsson, J. S. and Celius, H. K. 2005, “Monitoring of Deposits in Pipeline using Pressure Pulse Technology”, Proceedings of the Fifth International Conference on Gas Hydrate, June 12- 16, 2005. Trondheim, Norway.

Guo et al. 2005 “ Flow Assurance” Offshore pipeline, Elsevier Publication, pp 175 – 194 the link is; <http://www.knovel.com/knovel2/Toc.jsp?BookID=1258&VerticalID=0>

Haaland S.E., “Simple and Explicit Formulas for the Friction factor in Turbulent Pipe Flow,” J. Fluid Eng., March 1983, pp. 89- 90

Hernan, A. M et al., 2000”Tracer Dispersion in a percolation Network with Spatial correlations”, The American Physical Society, Volume 61, Number 1.

Hirschberg, A. et al. 1984 “Influence of Temperature and Pressure on Asphaltene Flocculation” SPE Journal, June 1984.

Hsu, J. J. C. et al. 1995 ”Wax Deposition Measurement and Scale-up Modeling for Waxy Live Crudes Under Turbulent Flow Conditions, SPE 29976, pp 242

Makgon, Y. F. 1997, “Hydrates of Hydrocarbons in PennWell Publisher”, Tulsa, Oklahoma

Marlin, T. 2006, “Instrumentation for Process Control” McMaster University.

Link; http://www.pc-education.mcmaster.ca/instrumentation/go_inst.htm

Meray, V. R. et al. 1993” Influence of Light Ends on the Onset Crystallization Temperature of Waxy Crudes Within the frame of Multiphase Transport”, Presented at the 68th Annual Technical Conference and Exhibition of the Society of Petroleum Engineers.

Mike, C et al., 1999 “Fighting Scale – Removal and Prevention”, Oilfield Review. Link; www.slb.com/media/services/resources/oilfieldreview/ors99/aut99/fighting.pdf

Rieckermann, J., Neumann, M., Ort, C., Huisman, J. L., and Gujer, W. 2004, "Dispersion Coefficients of sewers from tracer experiments" International conference on urban drainage modeling, Dresden, pp 417- 426

Riquarts H. P., "A Physical Model for Axial Mixing of the Liquid Phase for Heterogeneous flow Regime in Bubble Columns. " Ger Chem. Eng., 4, 18-23 (1981).

Stalkup, F.I. Jr.: Miscible Displacement, Monograph Series, SPE, Richardson, TX (1983) **8**.

Sushil, K. S et al., 2003, "Dispersion Coefficient of Stream from Tracer Experiment data", Journal of Environmental Engineering ASCE June 2003, pp 543

Svein, M. S and Jon, K, 1992 "Recent Advances in Improved Oil Recovery Methods for North Sea Sandstone Reservoirs" Spor Monograph, Norwegian Petroleum Directorate, Stavanger.

Taylor, G. I. (1954) "The Dispersion of matter in turbulent flow through a pipe", proceeding Royal Society. (London), Series A, 223: 446 – 468

Taylor, G. I. 1953, "Dispersion of soluble matter in solvent flowing slowly through a tube". Proceeding Royal Society (London), Series A, 219: 186 – 203

US EPA, "Dispersion and Exchanges" the link is;

<http://www.epa.gov/ATHENS/wwqtsc/courses/wasp7/transport/Dispersion.ppt>

Wang, J. X. et al. 2003, "Anticipating Asphaltene Problems Offshore a Practical Approach", Presented at the 2003 OTC Conference, Houston.

LISTS OF FIGURES AND TABLES:

Figures:

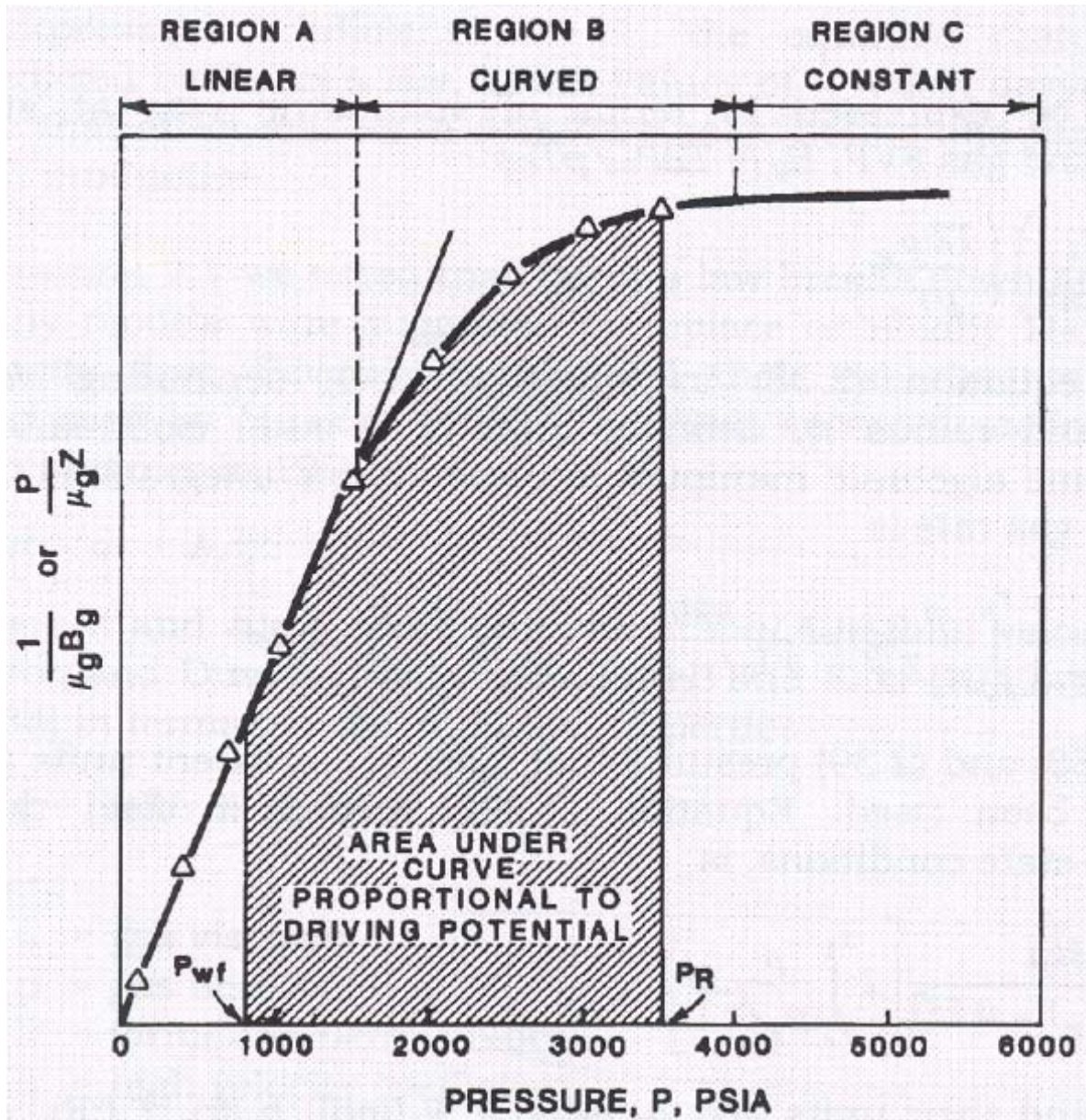


Figure 1 Gas Pressure Function Curve (Golan 1996), pp 135

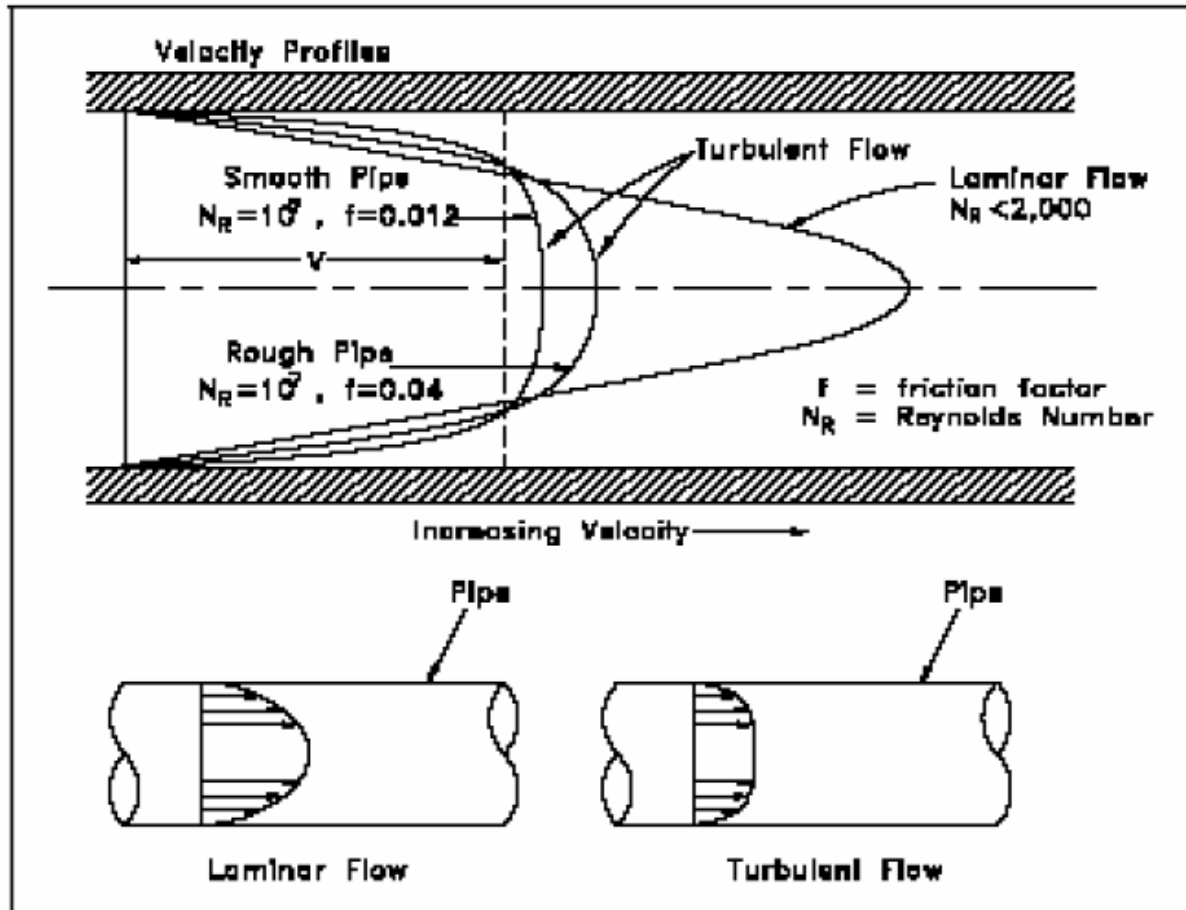


Figure 2 A typical velocity profiles for laminar and turbulent flow (Sources Engineers Edge site)

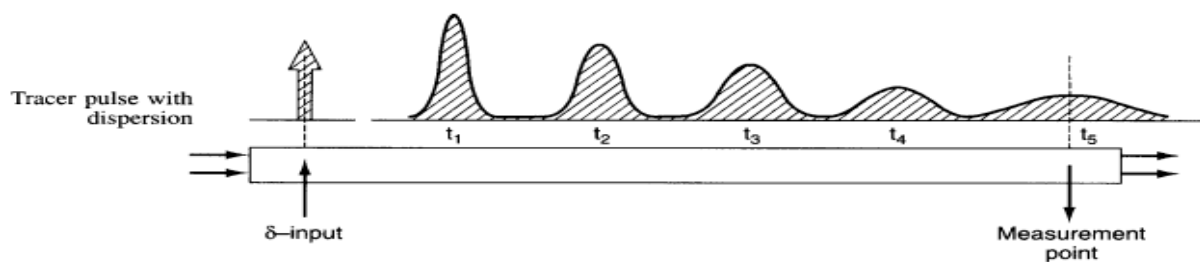


Figure 3 Tracer Distribution Pattern in a pipeline

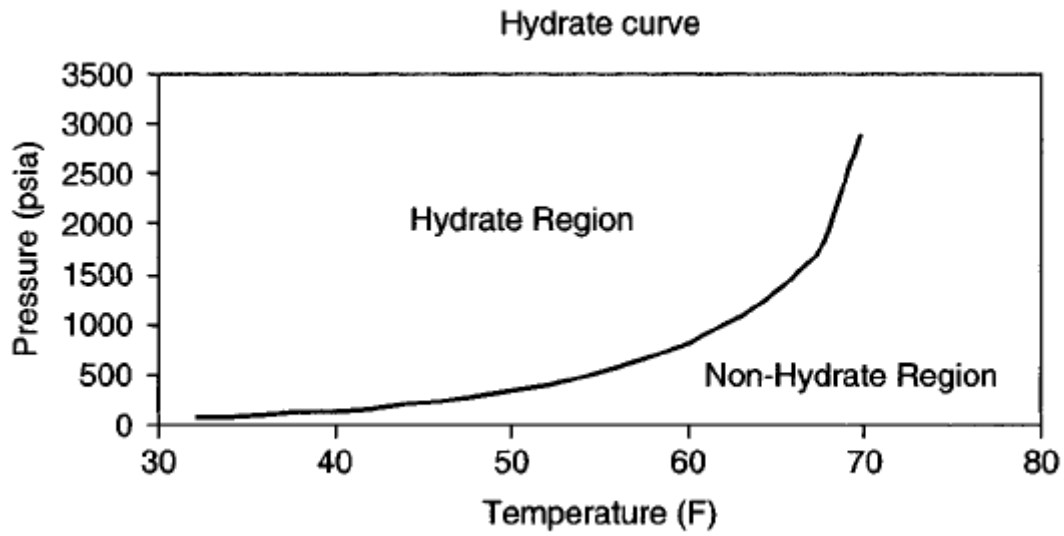


Figure 4 Hydrate formation curve (Guo et al., 2005)

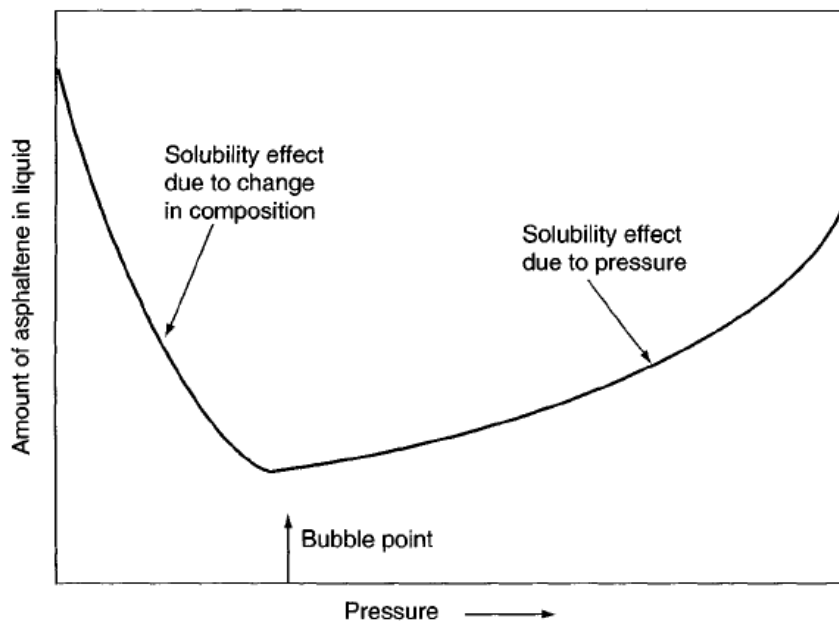


Figure 5 Amount of Asphaltene Precipitated as a function of Pressure (Guo et al., 2005)

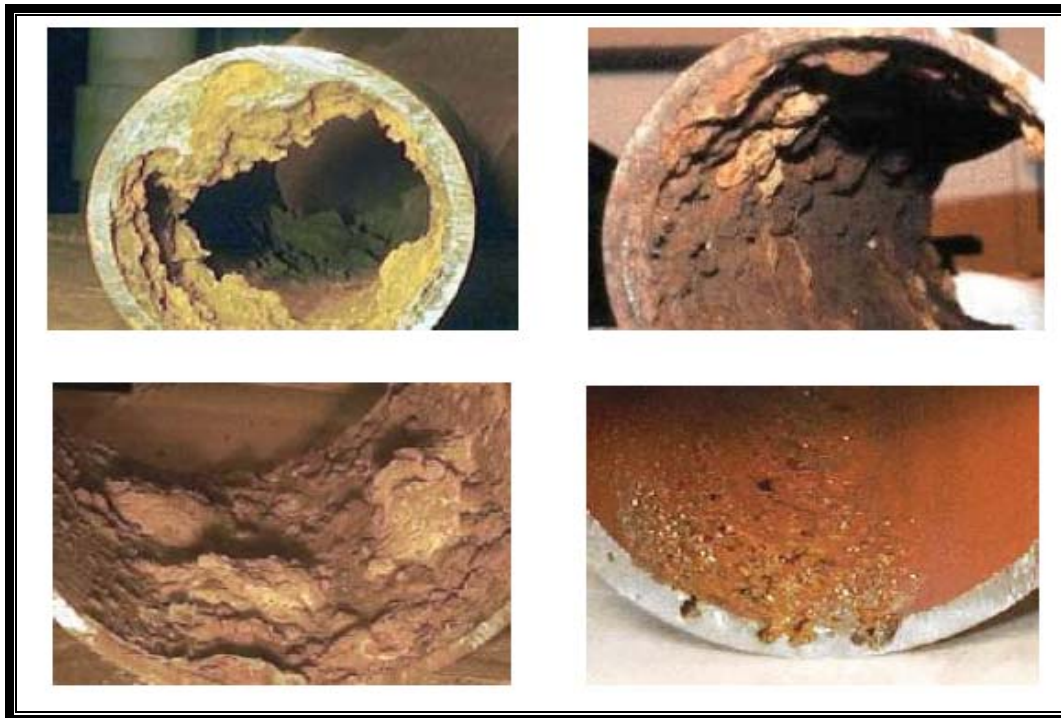


Figure 6 A Typical Deposits layer in Pipeline

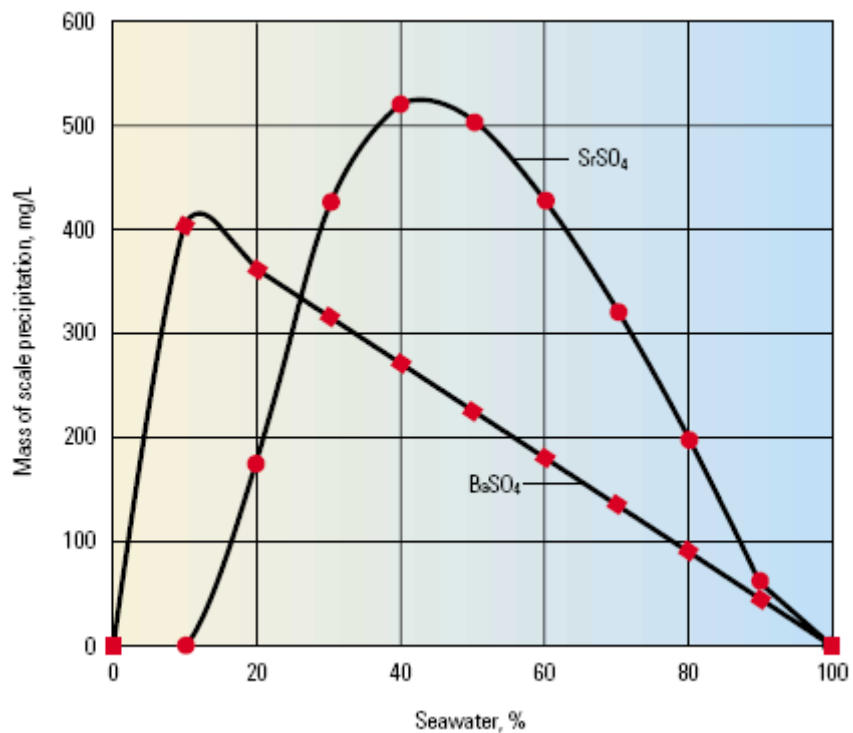


Figure 7 Amount of Scale Precipitated from mixture of Seawater and Formation water. (Mike et al., 1999), pp 34

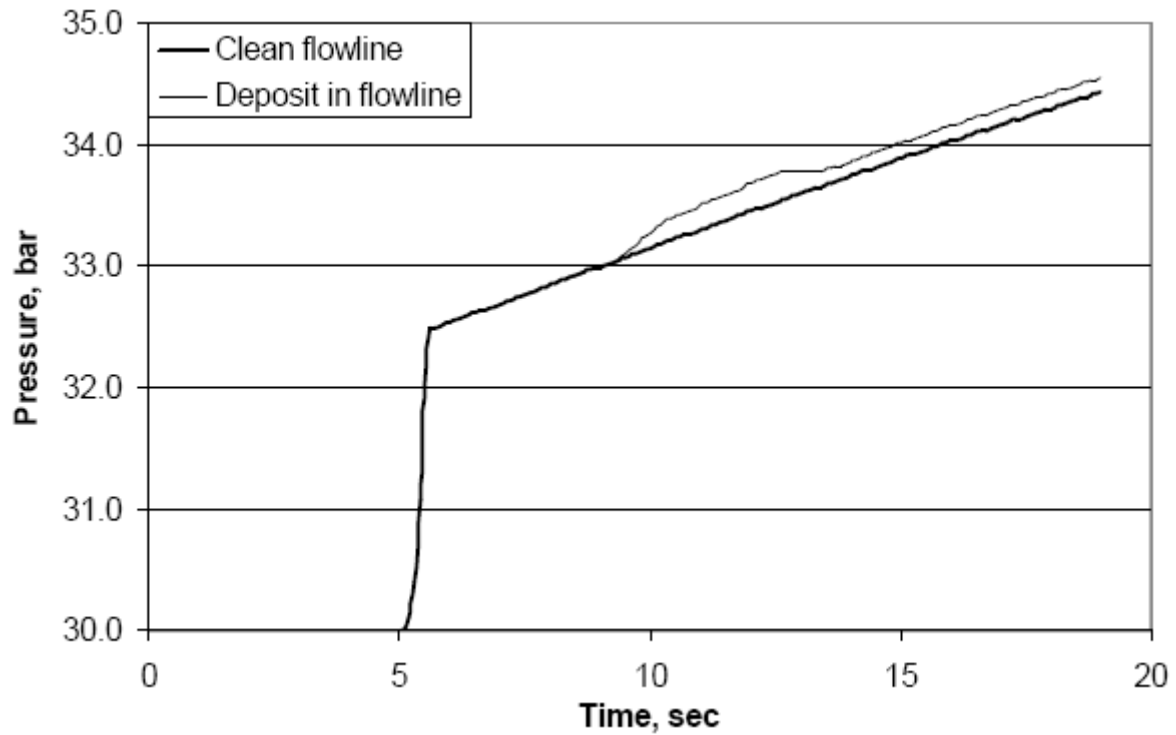


Figure 8 Pressure Pulse Response for clean Pipe (solid line) and Pipe with Deposits (thin line) (Gudmundsson and Celius, 2005)



Figure 9 Pipeline sections showing different deposits spread

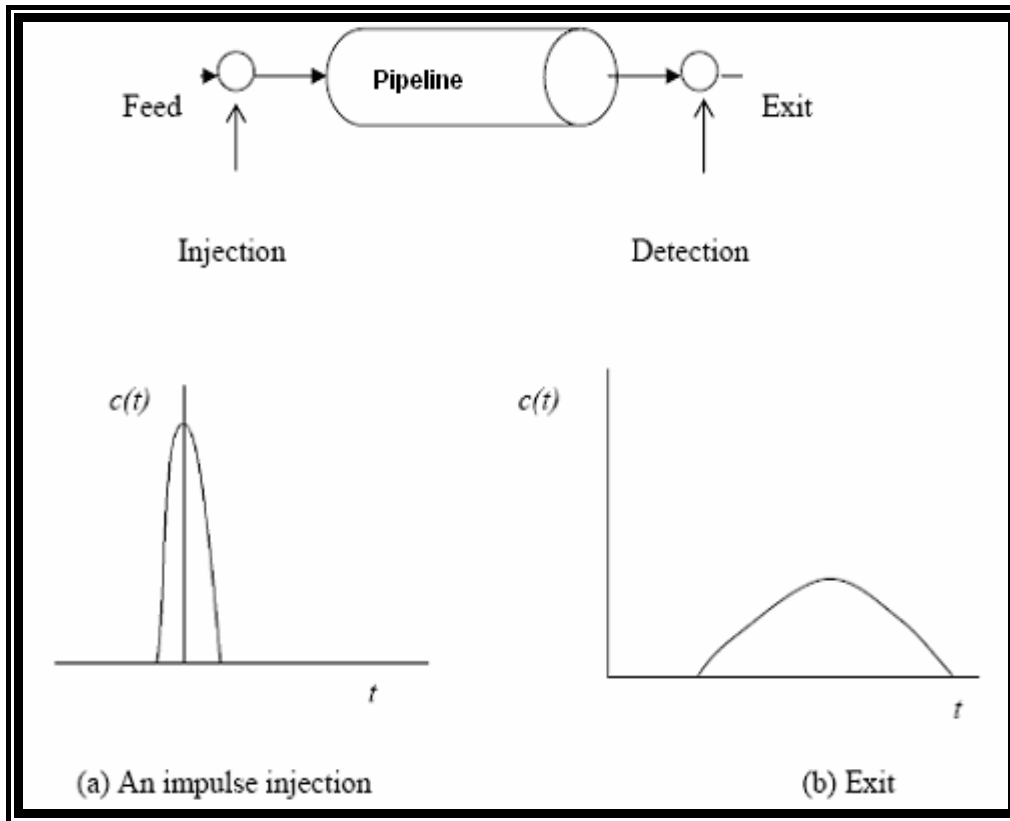


Figure 10 Tracer Response at the Inlet and Outlet of a pipeline

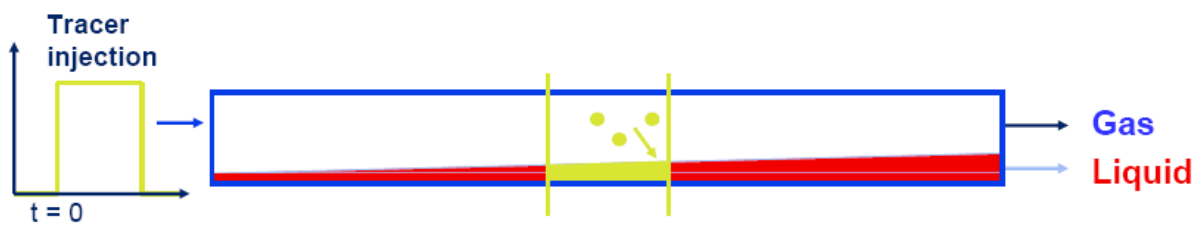


Figure 11 Tracer Flow in Pipeline with Multiphase Fluid (Bjørnar 2005)



Figure 12 Tracer Response in Multiphase pipeline (Bjørnar 2005)



Figure 13 Pipeline with an undulating path (Bjørnar 2005)

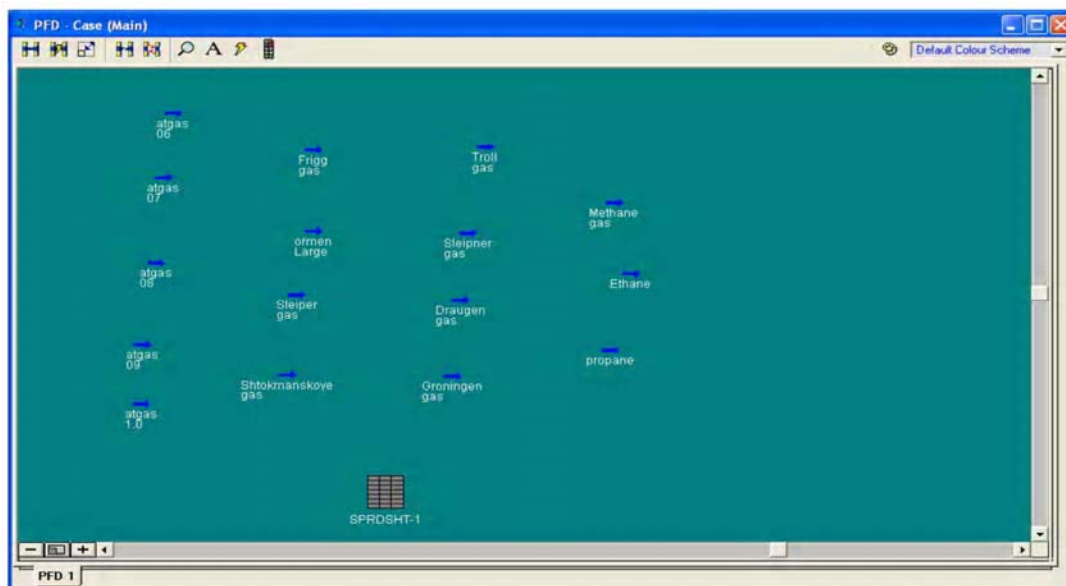


Figure 14 HYSYS Simulation Model Window for the pressure function

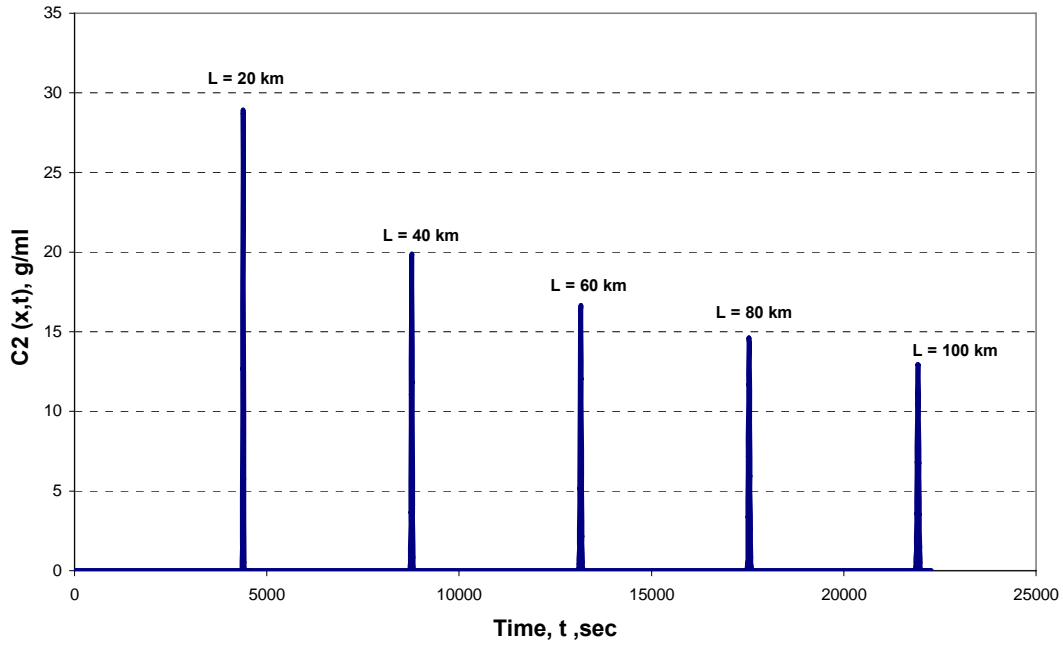


Figure 15 Tracer Concentration Profile at Different Location for a uniform 8'' (ID) Pipe

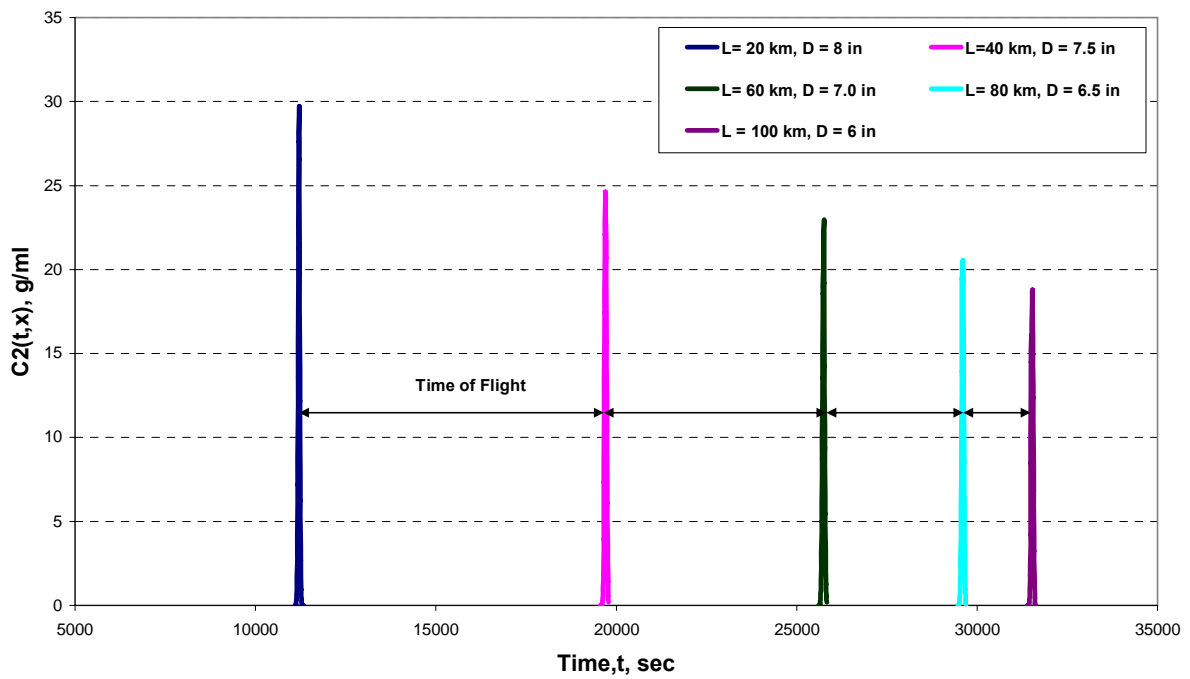


Figure 16 Tracer Concentration Profile at Different Locations with Different Pipe diameters

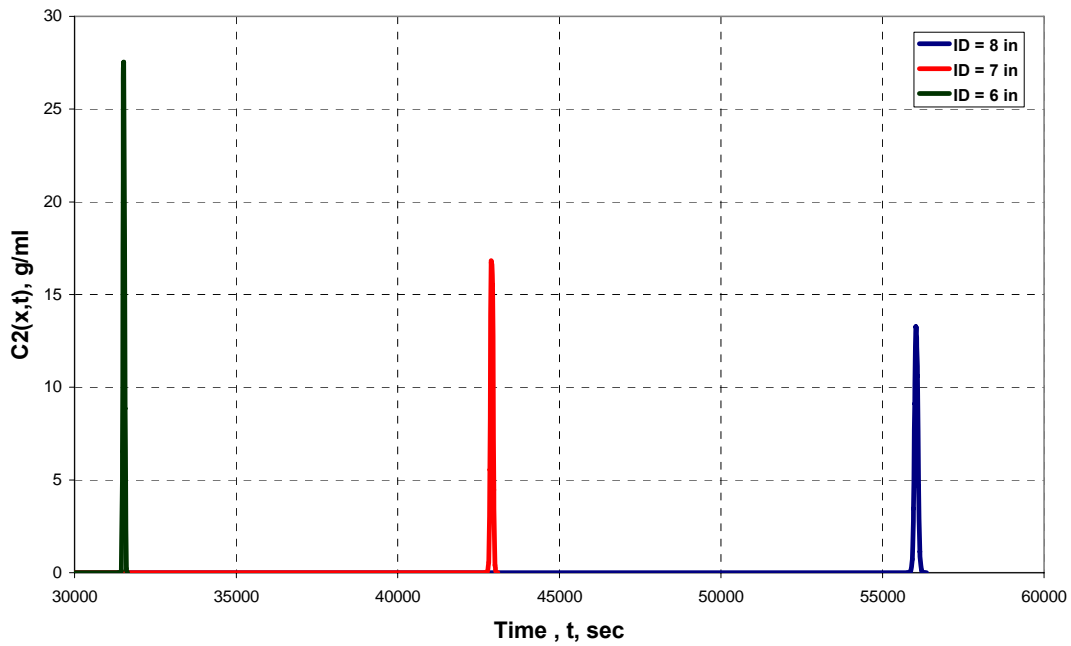


Figure 17 Tracer Pulses at the exit of the pipelines (100 km) with Different ID pipe

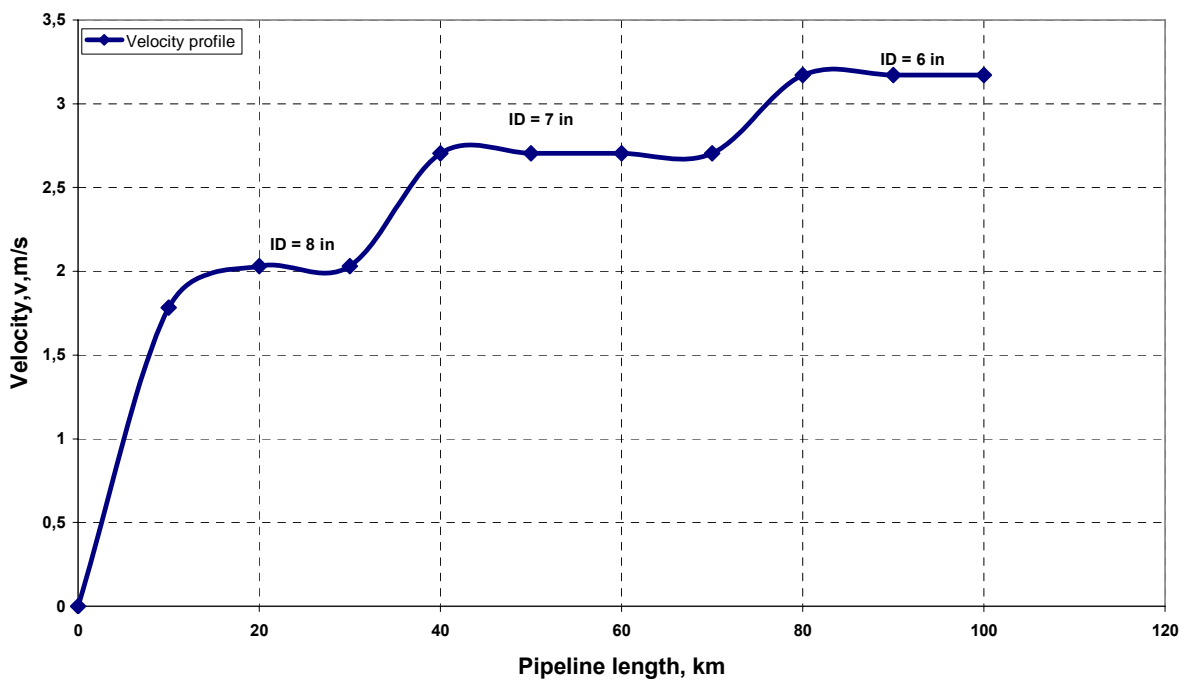


Figure 18 Effect of Pipe Diameter on Tracer Velocity Profile

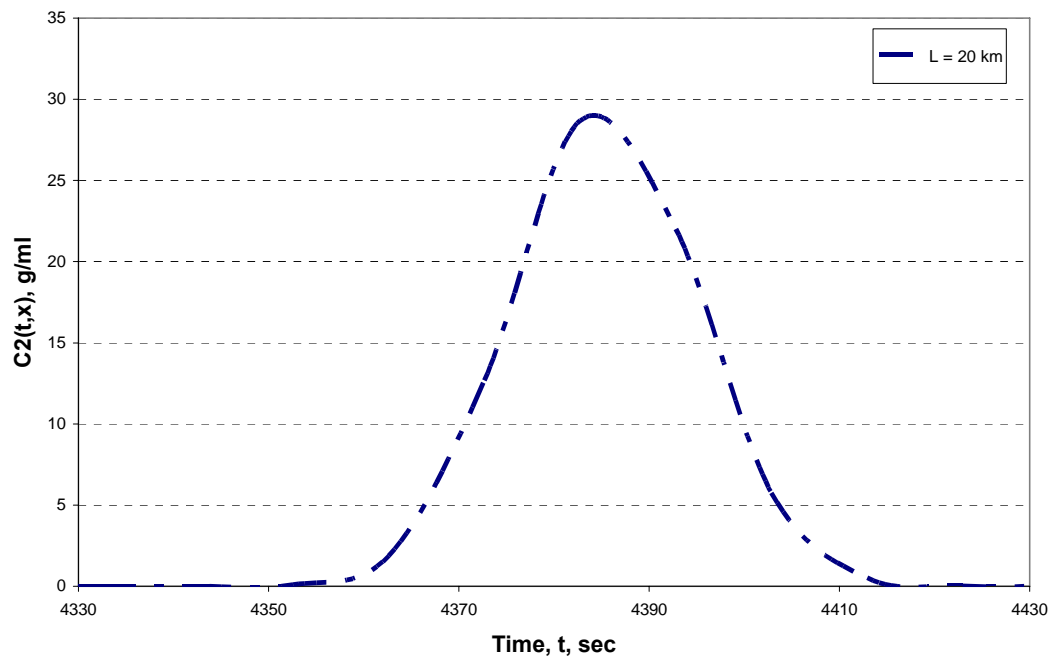


Figure 19 A Tracer Concentration Profile at 20 km Downstream of Injection Point.

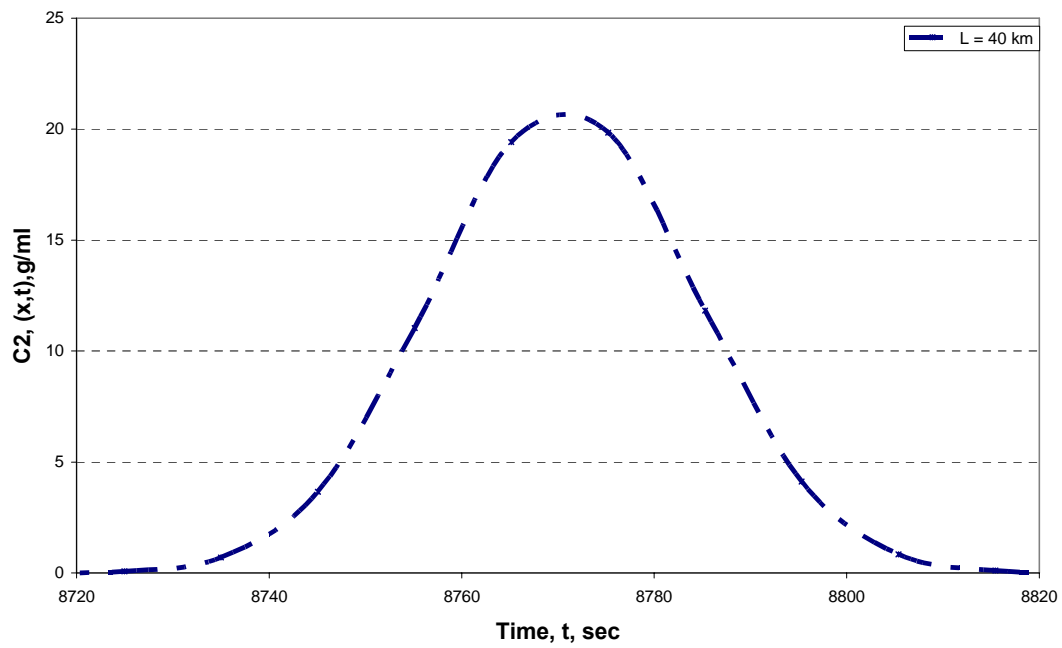


Figure 20 A Tracer Concentration Profile at 40 km Downstream of Injection Point.

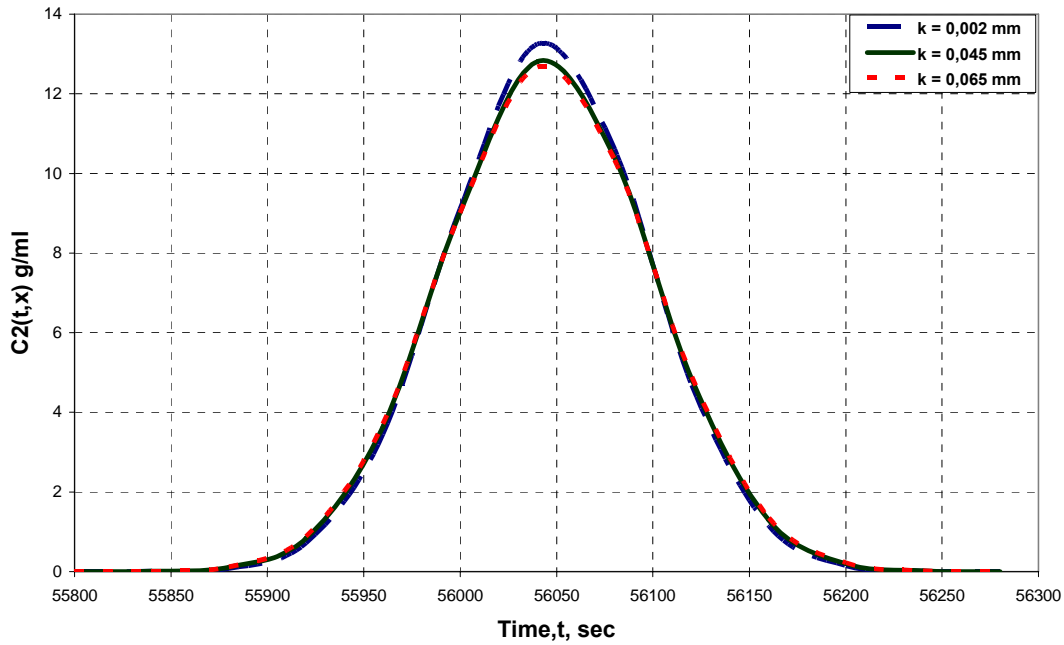


Figure 21 Effect of Pipe Roughness on Tracer Dispersion for 8 inches ID Pipeline

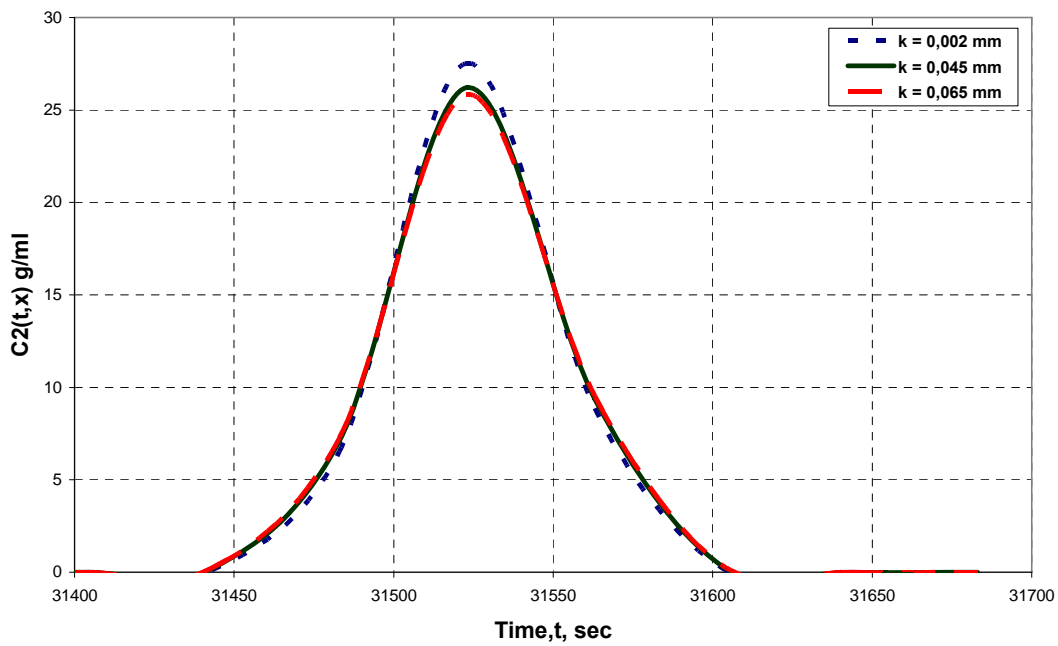


Figure 22 Effect of Pipe Roughness on Tracer Dispersion for 6 inches ID Pipeline

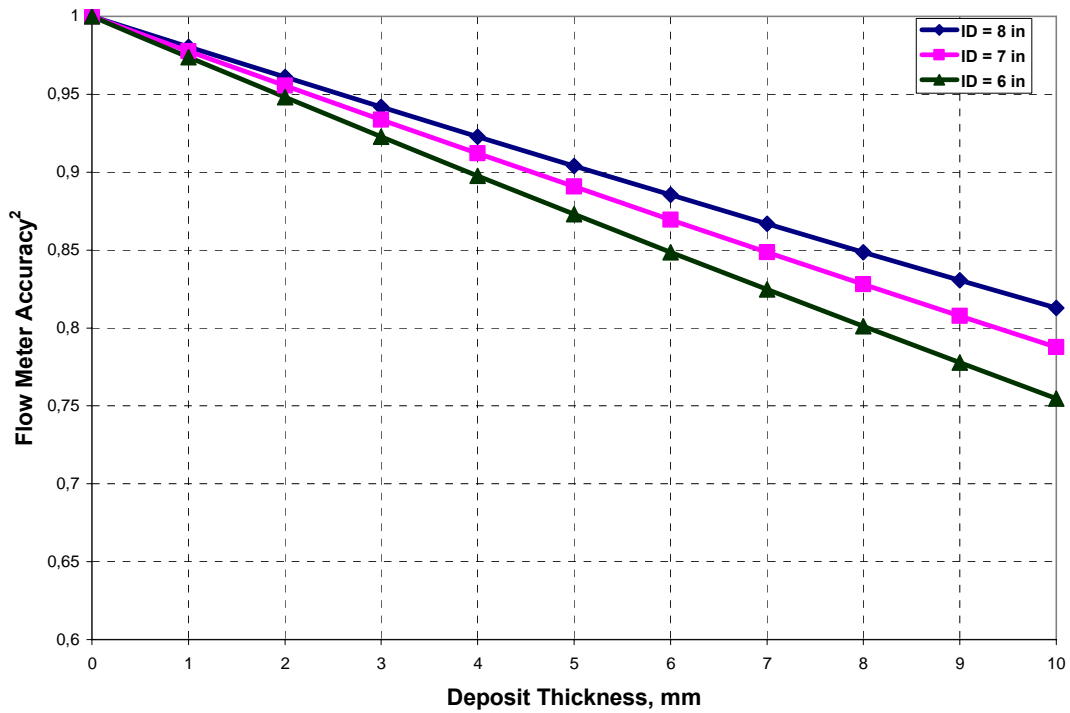


Figure 23 Flow Meter Accuracy with Deposits Thickness

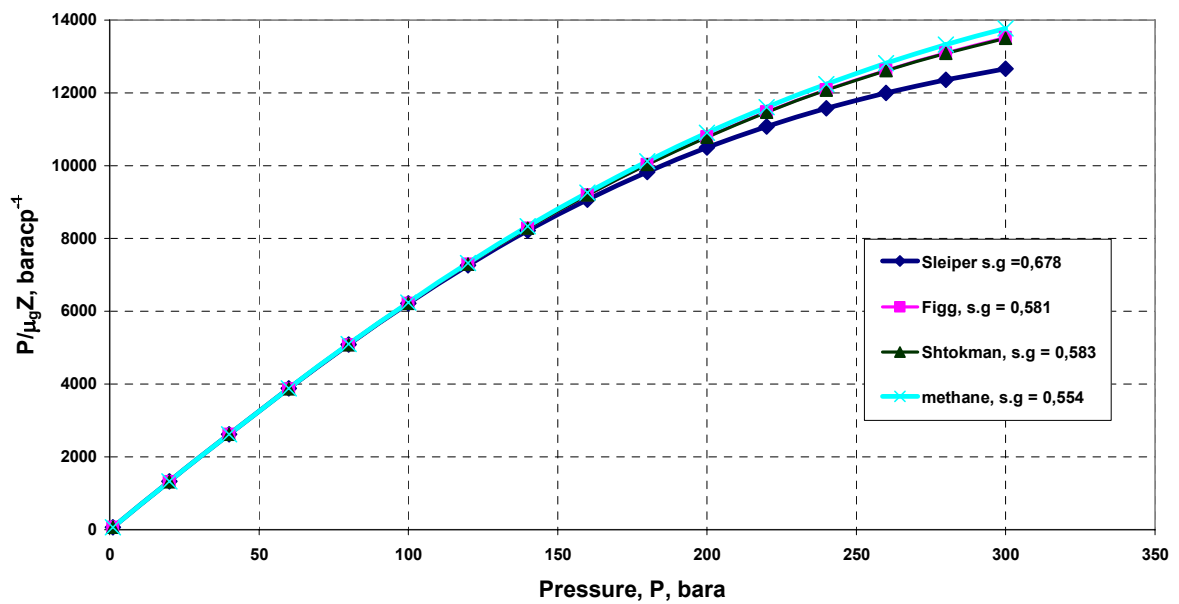


Figure 24 Pressure Function of Produced gases and Methane for different Fields

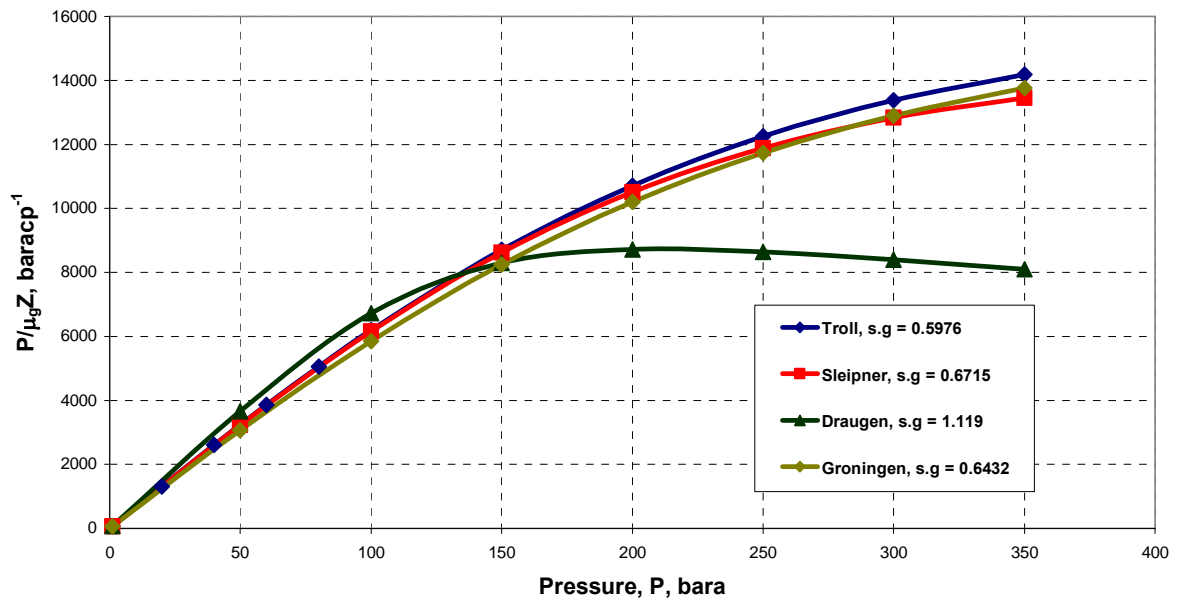


Figure 25 Pressure Function of Processed gases for different Fields

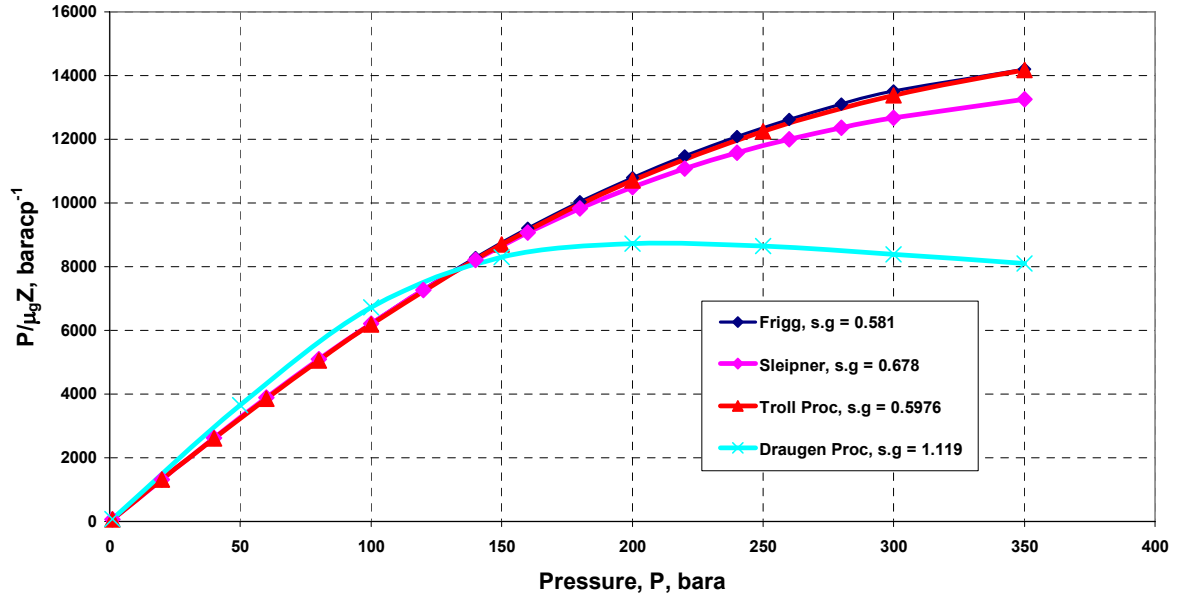


Figure 26 Comparison of Pressure Function of Produced and Processed Gas

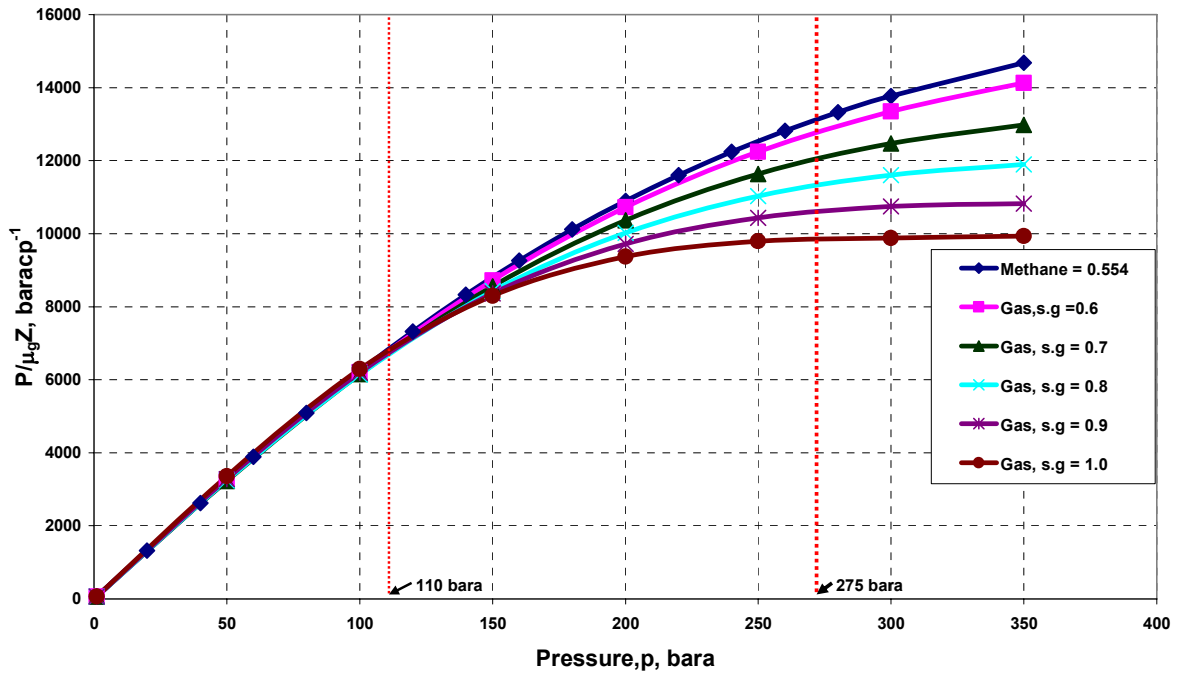


Figure 27 Effect of Gas Gravity on Pressure Function

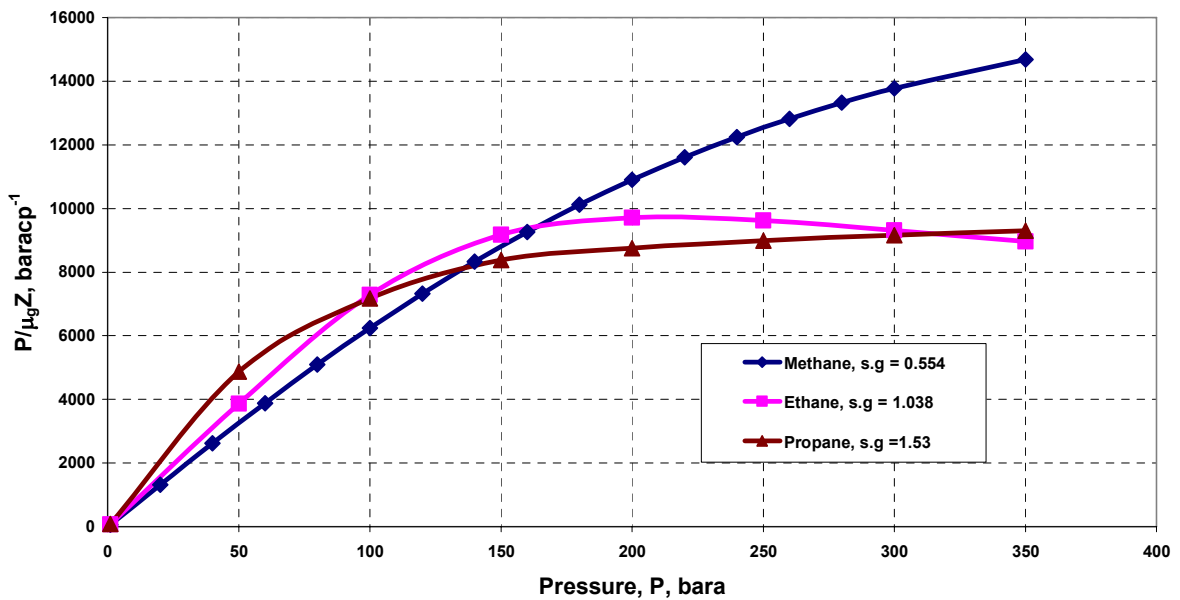


Figure 28 pressure Function for Methane, Ethane, and Propane

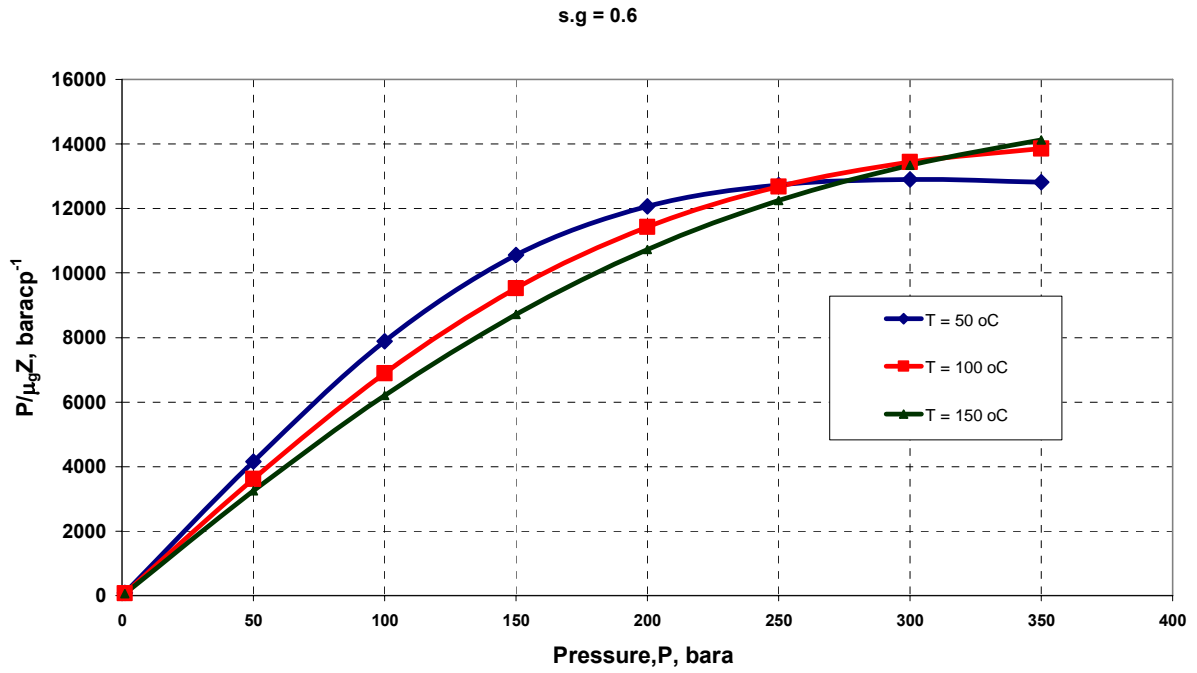


Figure 29 Effect of Temperature on Pressure function of gas with s.g = 0.6

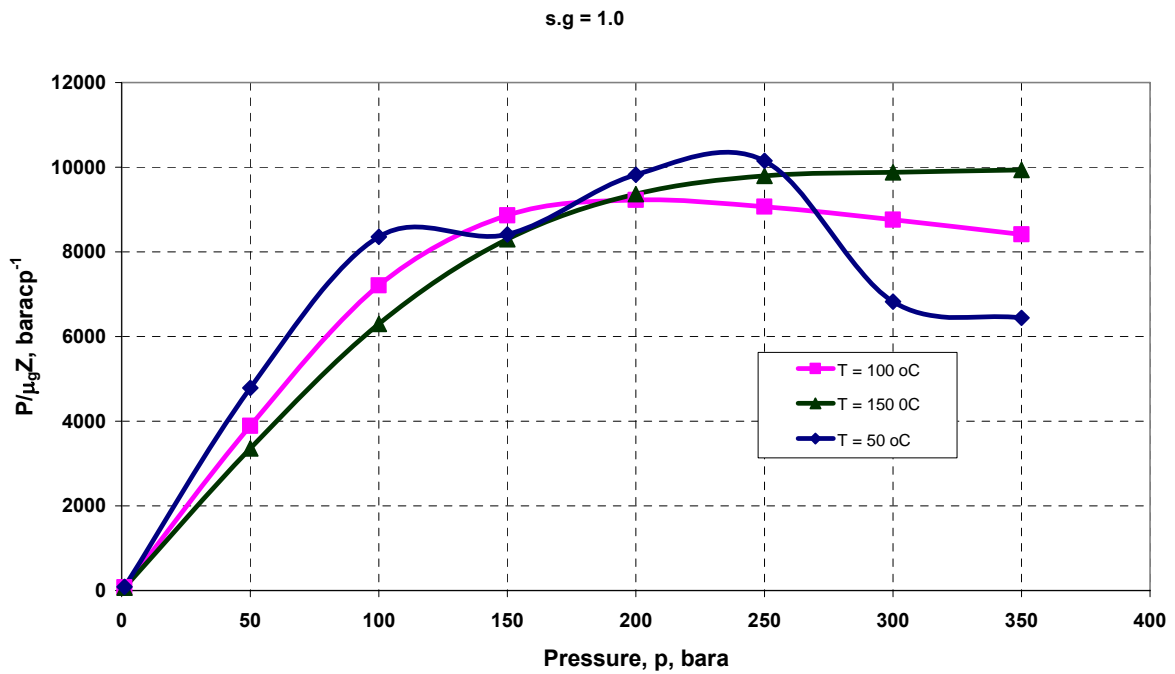


Figure 30 Effect of Temperature on Pressure function of gas with s.g = 1.0

Tables:

Table 2 Flow Rate Accuracy for Different Flow Meters (Marlin 2006)

Sensor	Rangeability ¹	Accuracy ²	Dynamics (s)	Advantages	Disadvantages
orifice	3.5:1	2-4% of full span	-	-low cost -extensive industrial practice	-high pressure loss -plugging with slurries
venturi	3.5:1	1% of full span	-	-lower pressure loss than orifice -slurries do not plug	-high cost -line under 15 cm
flow nozzle	3.5:1	2% full span	-	-good for slurry service -intermediate pressure loss	-higher cost than orifice plate -limited pipe sizes
elbow meter	3:1	5-10% of full span	-	-low pressure loss	-very poor accuracy
annubar	3:1	0.5-1.5% of full span	-	-low pressure loss -large pipe diameters	-poor performance with dirty or sticky fluids
turbine	20:1	0.25% of measurement	-	-wide rangeability -good accuracy	-high cost -strainer needed, especially for slurries
vortex shedding	10:1	1% of measurement	-	-wide rangeability -insensitive to variations in density, temperature, pressure, and viscosity	-expensive
positive displacement	10:1 or greater	0.5% of measurement	-	-high reangeability -good accuracy	-high pressure drop -damaged by flow surge or solids

Table 3 Frigg Produced gas Composition (Maritvold, 1990).

Components	Mole % Fraction
N ₂	0.3599
CO ₂	0.2902
C1	95.5225
C2	3.6887
C3	0.0379
i-C4	0.0085
n-C4	0.0047
i-C5	0.0041
n-C5	0.0004
C6	0.0049
C7	0.0030
C8	0.0055
C9	0.0050
C10	0.0123
C11	0.0145
C12	0.0173
C13	0.0097
C14	0.0031
C15	0.0026
C16	0.0019
C17	0.0012
C18	0.0017

Table 4 Sleipner Produced gas Composition (Gudmundsson Lecture note, 2005)

Components	Mole % Fraction
N ₂	1.467
CO ₂	0.260
C1	83.995
C2	10.657
C3	3.123
i-C4	0.216
n-C4	2.238
i-C5	0.025
n-C5	0.016
C6	0.003
C7+	0.0000

Table 5 Shtokmanskoye Produced gas Composition (Gudmundsson 2006)

Components	Mole % Fraction
N ₂	1.3
CO ₂	0.5
C1	95.4
C2	1.7
C3	0.5
C4	0.26
C5+	0.34

Table 6 Processed Gas compositions Mole % for different gas Field
(Gudmundsson 2006)

Components	Troll Field (Norway)	Sleipner Field (Norway)	Draugen Field (Norway)	Groningen Field (Netherlands)
N ₂	1.657	0.745	0.738	14.32
CO ₂	0.319	3.429	0.720	0.89
C1	93.070	83.465	44.659	81.29
C2	3.720	8.653	13.64	2.87
C3	0.582	3.004	22.825	0.38
i-C4	0.346	0.250	4.875	0.15
n-C4	0.083	0.327	9.466	0.04
C5+	0.203	0.105	3.078	0.06
Total	100	100	100	100

Appendices

Appendix A: Tracer Concentration Response Calculation in pipeline.

The tracer concentration response in pipeline is generated from the velocity profile using the equation proposed by Taylor (1953) as shown in equation 1 below.

$$C(x,t) = \frac{M}{A\sqrt{4K\pi t}} \exp\left(-\frac{(x-ut)^2}{4Kt}\right) \dots\dots\dots 1a$$

Where $C(x,t)$ is the concentration of the tracer downstream of the injection point (g/ml), M is the mass of the tracer injected (gram), t is the time (s), u is the mean flow velocity (m/s), x distance downstream of the injection point (m), and K is the longitudinal dispersion coefficient (m²/s).

$$K = 5.05dv_* \dots\dots\dots 2a$$

Where d (m) is the pipe diameter and v_* is the shear velocity

$$v_* = \sqrt{\frac{f}{8}}v \dots\dots\dots 3a$$

Where the friction factor f is define as:

$$\sqrt{\frac{1}{f}} = -\frac{1.8}{n} \log\left[\left(\frac{6.9}{Re}\right)^n + \left(\frac{k}{3.75d}\right)^{1.11n}\right] \dots\dots\dots 4a$$

Where k is the pipe roughness, d (m) is the pipe diameter, and Re the Reynolds Number.

$$Re = \frac{\rho vd}{\mu} \dots\dots\dots 5a$$

ρ (kg/m³) is the fluid density, μ (pa.s) is the fluid viscosity, and v (m/s) is the fluid mean velocity in the pipe

The concentration response generated using the above procedure is shown in Table 9 below.

Table 7 Tracer Response Sample Calculation

Pipe Parameters				
Pipe Diameter	8	in	0,2032	m
Pipe Roughness	0,002	mm	0,000002	m
Pipe Length	100	km	100000	m
Pipe Area	0,03243348	m ²		
Fluid Parameters				
Fluid Density	720	kg/m ³		
Fluid Viscosity	0,7	Cp	0,0007	Pa.s
Fluid Flow Rate	5000	m ³ /d	0,05787037	m ³ /s
Mean Velocity	1,78427859	m/s		
Mass of tracer injected	100	g		
System Parameters				
Reynolds Number	372924,422			
Friction Factor	0,0138654			
Shear velocity	0,07428204			
Dispersion Coefficient	0,07622526			

Table 8 Concentration response at different locations along the pipeline

L = 20 km		L = 40 km		L = 60 km		L = 80 km		L = 100 km	
t	C2(x,t)	t	C2(x,t)	t	C2(x,t)	t	C2(x,t)	t	C2(x,t)
sec	g/ml	sec	g/ml	sec	g/ml	sec	g/ml	sec	g/ml
11100	0	19560	0	25605	0	29469	0	31397	0
11110	0,003	19570	0,0002	25615	0,0007	29479	0,0016	31407	0,0003
11120	0,0175	19580	0,0012	25625	0,0031	29489	0,0077	31417	0,0021
11130	0,0854	19590	0,0058	25635	0,0129	29499	0,0315	31427	0,0113
11140	0,3437	19600	0,024	25645	0,0475	29509	0,1127	31437	0,0512
11150	1,1439	19610	0,0864	25655	0,1542	29519	0,3522	31447	0,1967
11160	3,1507	19620	0,273	25665	0,4427	29529	0,9619	31457	0,6421
11170	7,1851	19630	0,7564	25675	1,1228	29539	2,2956	31467	1,7833
11180	13,5739	19640	1,8388	25685	2,5174	29549	4,7886	31477	4,213
11190	21,2535	19650	3,9229	25695	4,9892	29559	8,7318	31487	8,4687
11200	27,5951	19660	7,3457	25705	8,7422	29569	13,92	31497	14,4864
11210	29,7253	19670	12,0759	25715	13,5448	29579	19,4034	31507	16,0907
11220	26,5784	19680	17,4322	25725	18,5592	29589	19,6524	31517	16,1381
11230	19,736	19690	22,101	25735	20,4926	29599	20,217	31527	18,5788
11240	12,1766	19700	24,6143	25745	22,1143	29609	20,5174	31537	18,7777
11250	6,2453	19710	24,086	25755	22,8733	29619	19,1877	31547	14,9583
11260	2,6641	19720	20,7123	25765	19,1982	29629	13,6979	31557	12,3553
11270	0,9456	19730	15,6554	25775	14,2605	29639	8,5573	31567	6,8595
11280	0,2794	19740	10,403	25785	9,3759	29649	4,6788	31577	3,2448
11290	0,0688	19750	6,0785	25795	5,457	29659	2,2393	31587	1,3079
11300	0,0141	19760	3,1236	25805	2,8121	29669	0,9382	31597	0,4493
11310	0,0024	19770	1,412	25815	1,2832	29679	0,3442	31607	0,1316
11320	0,0003	19780	0,5616	25825	0,5185	29689	0,1106	31617	0,0329
11330	0,00021	19790	0,1965	25835	0,1856	29699	0,0311	31627	0,007

Appendix B: Flow Rate Sensitivity on Tracer Testing Calculation

The effect of deposits thickness on the pipeline area is calculated using the following procedures below. The deposits in the pipeline are assumed to be uniform around the pipeline diameter.

For a pipeline with deposit the effective internal diameter is calculated as;

$$d_{eff} = d_o - 2t \dots\dots\dots 1b$$

Where, d_o (mm) is the initial internal diameter before deposit, d_{eff} (mm) is the effective internal diameter, and t is the deposit thickness.

Therefore the change in pipeline area due to deposits is calculated as;

$$A_o = \frac{\pi d_o^2}{4} \dots\dots\dots 2b$$

Where A_o is the initial pipeline area

$$A_{eff} = \frac{\pi d_{eff}^2}{4} \dots\dots\dots 3b$$

Where A_{eff} is the effective pipeline area after the deposits.

Therefore change in the area due to deposit is calculated as:

$$\frac{A_{eff}}{A_o} = \frac{d_{eff}^2}{d_o^2} \dots\dots\dots 4b$$

Example:

Calculate the change in pipeline area with initial internal diameter of 8 inches (203.2 mm) with deposit of 2 mm thick.

Solution;

$$d_o = 203.2 \text{ mm and } t = 2 \text{ mm.}$$

$$d_{eff} = d_o - 2t$$

$$d_{eff} = 203.2 - 2(2)$$

$$d_{eff} = 203.2 - 4$$

$$d_{eff} = 199.2 \text{ mm}$$

Therefore change in area is

$$\begin{aligned} \frac{A_{eff}}{A_o} &= \frac{d_{eff}^2}{d_o^2} = \frac{(199.2)^2}{(203.2)^2} \\ &= 0.961 \equiv \text{Flow measurement accuracy}^2 \end{aligned}$$

Table 9 Calculation of changes in Pipeline Area with Deposit Thickness

	ID (8 in) (203.2 mm)	ID (7 in) (177.8 mm)	ID (6 in) (152.4 mm)
Deposit Thickness (mm)	%Δ A/Ao	%Δ A/Ao	%Δ A/Ao
0	1	1	1
1	0.980	0.978	0.974
2	0.961	0.956	0.948
3	0.942	0.934	0.923
4	0.923	0.912	0.898
5	0.904	0.891	0.873
6	0.885	0.869	0.849
7	0.867	0.849	0.824
8	0.849	0.828	0.801
9	0.831	0.808	0.778

Appendix C: Pressure Functions Calculations

The pressure functions generated from the HYSYS process simulator and Excel are shown in the Tables below:

Table 10 Pressure Function Calculation for Frigg gas and Methane

Frigg gas				Methane gas			
Pressure	Viscosity	S.G	0,581	Pressure	Viscosity	S:G	0,554
bara	cp	Z-factor	P/μ_gZ	bara	cp	Z-factor	P/μ_gZ
			bara/cp				bara/cp
1	0,01509	0,999	66,290	1	0,01504	0,999	66,521
20	0,01533	0,989	1319,759	20	0,01526	0,990	1323,731
40	0,01562	0,979	2615,917	40	0,01553	0,982	2623,176
60	0,01595	0,972	3872,895	60	0,01584	0,975	3883,828
80	0,01631	0,966	5077,595	80	0,01619	0,970	5093,589
100	0,01671	0,962	6219,419	100	0,01656	0,967	6242,711
120	0,01714	0,960	7290,378	120	0,01696	0,966	7323,832
140	0,01760	0,960	8285,103	140	0,01739	0,966	8331,957
160	0,01809	0,961	9200,704	160	0,01785	0,968	9264,312
180	0,01860	0,964	10036,496	180	0,01832	0,971	10120,127
200	0,01914	0,968	10793,190	200	0,01882	0,975	10900,298
220	0,01969	0,974	11473,831	220	0,01933	0,980	11607,035
240	0,02027	0,980	12082,164	240	0,01986	0,987	12243,582
260	0,02085	0,988	12622,614	260	0,02041	0,994	12813,884
280	0,02146	0,996	13100,014	280	0,02096	1,003	13322,318
300	0,02207	1,006	13519,709	300	0,02153	1,012	13773,476

Table 11 Pressure Function Calculation for Sleipner gas Field and Shtokman Field

Sleipner gas				Shtokman gas			
Pressure	Viscosity	S:G	0,678	Pressure	Viscosity	S:G	0,583
bara	cp	Z-factor	P/μ_gZ	bara	cp	Z-factor	P/μ_gZ
			bara/cp				bara/cp
1	0,01511	0,999	66,245	1	0,01510	0,999	66,286
20	0,01539	0,983	1322,042	20	0,01533	0,989	1319,738
40	0,01575	0,968	2624,029	40	0,01562	0,979	2615,929
60	0,01616	0,956	3885,324	60	0,01595	0,971	3872,930
80	0,01662	0,946	5087,897	80	0,01632	0,966	5077,581
100	0,01713	0,939	6216,864	100	0,01672	0,962	6219,234
120	0,01768	0,935	7261,060	120	0,01715	0,960	7289,862
140	0,01828	0,932	8213,330	140	0,01761	0,960	8284,072
160	0,01892	0,932	9069,983	160	0,01810	0,961	9198,973
180	0,01959	0,934	9830,728	180	0,01862	0,964	10032,092
200	0,02030	0,938	10498,641	200	0,01916	0,968	10787,313
220	0,02103	0,944	11079,001	220	0,01971	0,973	11466,261
240	0,02179	0,951	11578,426	240	0,02029	0,980	12072,749
260	0,02256	0,960	12004,228	260	0,02088	0,987	12611,304
280	0,02335	0,970	12363,929	280	0,02148	0,996	13086,876
300	0,02416	0,980	12664,897	300	0,02210	1,005	13504,584

Table 12 Pressure Function Calculated Results for Ethane and Propane

Ethane				Propane			
MW = 30,070		S.G = 1,038		MW = 44,097		S.G = 1,530	
Pressure	Viscosity	Z-factor	P/ $\mu_g Z$	Pressure	Viscosity	Z-factor	P/ $\mu_g Z$
bara	cp		bara/cp	bara	cp		bara/cp
1	0,01335	0,997	75,119	1	0,01176	0,994	85,542
50	0,01492	0,866	3870,529	50	0,01509	0,679	4879,265
100	0,01790	0,767	7287,743	100	0,02851	0,489	7170,999
150	0,02250	0,727	9172,266	150	0,03254	0,550	8377,484
200	0,02786	0,739	9707,090	200	0,03548	0,644	8747,571
250	0,03333	0,780	9617,707	250	0,03744	0,743	8985,641
300	0,03862	0,834	9317,673	300	0,03890	0,842	9159,035
350	0,04370	0,893	8965,158	350	0,04006	0,940	9294,248

Table 13 Gas Composition with Different Specific Gravity

Components	Mole Fractions				
	gas, s,g = 0.6	gas, s,g = 0.7	gas, s,g = 0.8	gas, s,g = 0.9	gas, s,g = 1.0
Comp Mole Frac (Nitrogen)	0,0054	0,017	0,0306	0,0403	0,0506
Comp Mole Frac (CO2)	0,0047	0,015	0,0269	0,0354	0,0445
Comp Mole Frac (Methane)	0,9452	0,8265	0,7115	0,5892	0,4599
Comp Mole Frac (Ethane)	0,022	0,0696	0,1128	0,1649	0,2309
Comp Mole Frac (Propane)	0,0096	0,0305	0,0436	0,0721	0,0907
Comp Mole Frac (i-Butane)	0,0082	0,0259	0,0466	0,0614	0,0771
Comp Mole Frac (n-Butane)	0,0041	0,0129	0,0232	0,0306	0,0385
Comp Mole Frac (i-Pentane)	0,0008	0,0026	0,0047	0,0062	0,0078
Comp Mole Frac (n-Pentane)	0,0000	0,0000	0,0000	0,0000	0,0000
Total Fraction	1.0	1.0	1.0	1.0	1.0

Table 14 Pressure Function Calculation for Formulated Gas Compositions

MW = 17,379		S.G = 0,600		MW = 20,277		S,G = 0,700	
Pressure	Viscosity	Z-factor	P/μ _g Z	Pressure	Viscosity	Z-factor	P/μ _g Z
bara	cp		bar/cp	bara	cp		bar/cp
1	0,01512	0,999	66,160	1	0,01524	0,999	65,674
50	0,01583	0,973	3245,383	50	0,01610	0,961	3232,370
100	0,01681	0,959	6205,805	100	0,01731	0,938	6157,328
150	0,01799	0,956	8718,258	150	0,01882	0,931	8559,173
200	0,01935	0,964	10722,666	200	0,02057	0,938	10366,115
250	0,02084	0,980	12243,588	250	0,02250	0,955	11631,370
300	0,02243	1,002	13345,210	300	0,02453	0,981	12464,794
350	0,02407	1,030	14122,227	350	0,02663	1,012	12979,172

MW = 23,170		S.G = 0,800		MW = 26,068		S.G = 0,900	
Pressure	Viscosity	Z-factor	P/μ _g Z	Pressure	Viscosity	Z-factor	P/μ _g Z
bara	cp		bara/cp	bara	cp		bara/cp
1	0,01529	0,999	65,485	1	0,01516	0,998	66,067
50	0,01631	0,948	3236,117	50	0,01636	0,931	3283,432
100	0,01780	0,915	6138,469	100	0,01820	0,887	6196,558
150	0,01969	0,904	8426,287	150	0,02062	0,870	8361,070
200	0,02192	0,910	10023,054	200	0,02348	0,877	9711,930
250	0,02436	0,931	11030,057	250	0,02659	0,901	10433,311
300	0,02692	0,960	11605,729	300	0,02980	0,937	10746,986
350	0,02953	0,997	11891,142	350	0,03303	0,979	10818,920

MW = 28,977		S.G = 1.000		(Methane) MW = 16,040		S.G = 0.554	
Pressure	Viscosity	Z-factor	P/μ _g Z	Pressure	Viscosity	Z-factor	P/μ _g Z
bara	cp		bara/cp	bara	cp		bara/cp
1	0,01494	0,998	67,066	1	0,01504	0,999	66,521
50	0,01634	0,912	3356,177	50	0,01584	0,975	3883,828
100	0,01861	0,854	6294,609	100	0,01656	0,967	6242,711
150	0,02171	0,832	8302,894	150	0,01739	0,966	8331,957
200	0,02537	0,841	9368,842	200	0,01882	0,975	10900,298
250	0,02928	0,872	9797,790	250	0,02041	0,994	12813,884
300	0,03324	0,914	9874,967	300	0,02153	1,012	13773,476
350	0,03716	0,949	9930,000	350	0,02299	1,037	14680,959